Physiologically based Pharmacokinetic (PBPK) Modelling of Cisplatin in Rats and Humans

By

Hyunjin Park

A thesis

presented to the University Of Waterloo

in fulfillment of the

thesis requirement for the degree of

Master of Science

in

Physics

Waterloo, Ontario, Canada, 2019

Author's declaration

I hereby declare that I am the sole author of this thesis. This is a true copy of the thesis, including any required final revisions, as accepted by my examiners.

I understand that my thesis may be made electronically available to the public.

Abstract

The physiologically based pharmacokinetic (PBPK) modelling has been accepted as one of the most effective mechanistic techniques to analyze pharmacokinetics (PK) of drugs in the drug development process. Its effectiveness in predicting the PK of drugs is important not only to the current drug development industry but also to potential growth of the pharmaceutical industry as it helps resolve ethical challenges.

The PK of cisplatin as an anticancer drug, and its metabolic disposition are investigated by proposing a PBPK modelling framework. A plausible PBPK model is developed to test and validate its predictive utility for extrapolation to other species with the drug. Building and testing a PBPK modelling workflow for translating from rat to human PK scenarios for cisplatin is particularly emphasized. Moreover, this workflow may be helpful to studying and understanding the PK of cisplatin analogues in future studies.

In this thesis, the PK of cisplatin is quantitatively studied by employing the PBPK modelling technique, and the modality of interspecies extrapolation from rat models to human models is then tested. As the metabolic mechanism of cisplatin is not evidently revealed, several assumptions have been made to successfully construct the PBPK model which would closely reproduce observed PK data of cisplatin for rats as well as for humans. Based on these assumptions, several parameters which define cisplatin ADME in an organism are reasonably selected. These parameters are optimized based on observed rat PK data by using a numerical optimization process. The PBPK model constructed based on the rat PK data is then evaluated by means of validating the optimized values of the parameters through comparing the PK simulations with other observed PK data for rats. Lastly, the validity of the model for the predictive performance on humans is assessed by translating the model into a human model and evaluating it based on observed PK data for humans.

Acknowledgements

I would like to express my deep and sincere gratitude to my supervisor, Dr. Qing-Bin Lu of Department of Physics at the University of Waterloo for giving me the opportunity to work on this project learning the pharmacokinetics of cisplatin and for his patience, enthusiasm and immense knowledge that led to the successful completion of my thesis. His expertise in study of cisplatin is invaluable throughout the thesis work and I cannot be grateful enough for his continued support and advice.

I would also like to express special thanks to the team of Dr. Edginton (Dr. Andrea Edginton, and Dr. Paul Malik) from the School of Pharmacy at the University of Waterloo for providing me the pharmaceutical knowledge and the modelling tools to perform the simulations. I would also like to thank Dr. Anton Burkov and Dr. Kesen Ma for kindly serving on my committee.

I am sincerely thankful to them for helping lead me to the new findings. This accomplishment would not have been possible without their supports.

Table of Contents

List of Figures

List of Tables

Chapter 1 Introduction

1.1 Chemotherapeutic Anticancer Drug, Cisplatin
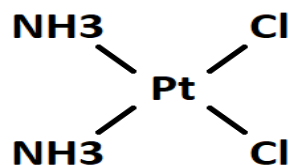
Figure 1: Illustration of the chemical structure of cisplatin

Cisplatin, or cis-diamminedichloroplatinum(II) (CDDP, $Pt(NH_3)_2Cl_2$,) is the first and most widely used platinum-based chemotherapy drug. US Food and Drug Administration (FDA) granted approval of cisplatin for testicular and ovarian cancer treatments in 1978 [1]. It is now the cornerstone agent in treating a variety of cancer, including ovarian cancer, testicular cancer, cervical cancer, bladder cancer, breast cancer, lung cancer, head and neck cancer, lymphomas cancer, brain tumors, germ cell tumors, malignant pleural mesothelioma and neuroblastoma [2], [3], [4]. Cisplatin has revolutionized treatments of many types of solid tumors. In particular, chemotherapy treatment with cisplatin shows very high response and cure rates for testicular tumors [5]. It is given into a patient intravenously (IV) and is commonly used with other drug(s) in combination chemotherapy or with radiotherapy.

Cisplatin is one of the most popular alkylating agents as it effectively disrupts the DNA function and causes cancer cell death by adding an alkyl group to the DNA base (mainly guanine, G base). The high binding affinity of cisplatin to the G base can be explained by the preferential electron transfer from the G base to cisplatin [6]. Electron transfer or dissociative electron transfer (DET) reaction is a reaction where electron transfer causes cleavage of chemical compound. The dissociation of chlorine ions from cisplatin and following alkylation preferentially to the G base can be demonstrated by the DET reaction of cisplatin occurring in the electron-rich G base:

$$e^- + Pt(NH_3)_2Cl_2 \Rightarrow [Pt(NH_3)_2Cl_2]^{*-} \Rightarrow Pt(NH_3)_2Cl^{\bullet} + Cl^- \quad (1)$$

$$e^- + Pt(NH_3)_2Cl \Rightarrow [Pt(NH_3)_2Cl]^{*-} \Rightarrow Pt(NH_3)_2^{\bullet} + Cl^-$$
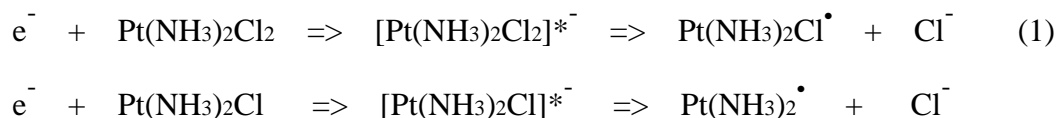
e^- represents an electron available from the DNA G base, and * and $^\bullet$ respectively denote that the compound is in an extremely short transient state, and the compound is a radical which is to be alkylated to the to the G base in this context.

Despite its effective cancer killing action, cisplatin-induced nephrotoxicity has been reported as a serious dose-limiting side effect in the anticancer treatment [7]. Consequently, there have been an enormous number of cisplatin-analogues synthesized over decades, aiming to minimize side effects while achieving effective treatment when compared with the treatment by cisplatin. However, only a very small portion of them have entered clinical trials and a few have been approved by the FDA to treat certain types of cancer.

Both efficacy and safety of the drug are of the utmost importance in the drug industry and are significantly influenced by many pharmacological factors such as drug permeability and tissue-to-plasma partition coefficients. Therefore, there is a compelling need to develop mechanistic tools and methods to achieve further pharmaceutical insight on the fate of the drug after it is administered to an organism.

1.2 Pharmacokinetics (PK) and Physiologically based Pharmacokinetic (PBPK) Modelling
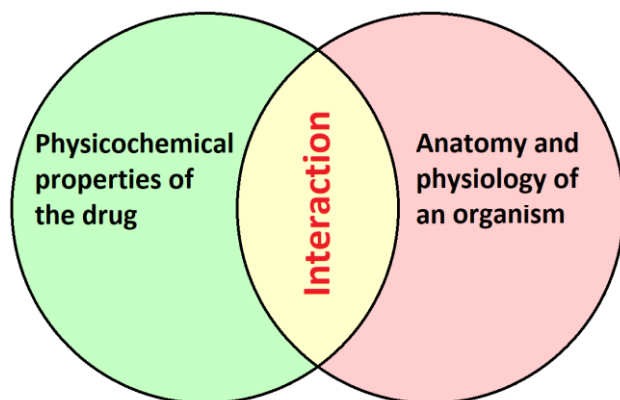
Figure 2: Illustration of how pharmacokinetics is defined

Pharmacokinetics (PK) is the study of the journey of an administered drug in a living organism and is useful in investigating the intensity of a drug's effectiveness or toxicity over time. The PK is accordingly defined by a drug's physicochemical properties and its interaction with the anatomy and physiology of an organism in terms of absorption, distribution, metabolism, and excretion (ADME) as illustrated in Figure 2. For example, two different PK profiles will be produced when two different individuals having different anatomical and physiological properties take the same drug with particular physicochemical properties. In the course of the modelling process adopted in this thesis, the interactions between the two systems (drug and organism) are represented by the ADME parameters such as intrinsic clearance, tissue-to-plasma partition coefficients, or fraction unbound.

Physiologically based pharmacokinetic (PBPK) modelling is a novel technique to build a mathematical model to predict and study the PK of drugs in organisms. The PBPK model provides a mechanistic representation of drug kinetics and generates simulations of the PK profiles by integrating the drug information with the anatomical and physiological system. As will be detailed in section 1.3, the PBPK model surpasses capabilities of empirical or classical compartmental models by accounting all major physiological and biochemical processes occurring in anatomical organ compartments connected via blood flow. It enables quantitative assessments of dispositions of several species in plasma under a variety of clinical settings which are essential in studying the PK of cisplatin, as will be elaborated throughout the thesis. It is widely used in the drug development process, as well as in pharmaceutical research [8].

In this thesis, a PBPK modelling technique is employed, in which a plausible rat model is firstly constructed, then evaluated based on observed PK datasets of rats, and finally translated into a human model; the latter is validated by comparing with observed PK datasets of humans. The convenient and practical use of the PBPK technique in translating from preclinical to clinical scenarios is carefully justified. In addition, the constructed model on one drug can be conveniently translated to predict and study the PK of other drugs as well, and this capacity may be explored in a future project.

1.3 Software used

In this thesis, open source platforms for the PBPK modelling, PK-Sim and MoBi v8.0 (www.open-systems-pharmacology.org) were used to construct and evaluate the PBPK model of cisplatin. PK-Sim provided an easy access to anatomical and physiological data for rats and humans, and enabled integrations of the data with input physicochemical data of cisplatin to perform numerous PK simulations [9]. MoBi was used to add several equations to generate new PK simulations that are not available by PK-Sim. To extract numerical PK data from plots in scientific literature, open source web-browser-based digitizing software, WebPlotDigitizer was used for a quick access to accurate data extraction [10].

1.4 PBPK Modelling of Cisplatin by '17 Compartment Model'

The whole body pharmacokinetics (PK) of cisplatin will be ascribed by a '17 compartment model' supported by the platforms PK-Sim and MoBi. The mechanistic PK process of cisplatin occurs in each of 17 anatomical organ compartments connected via physiological blood flow (indicated with arrows) to the systemic circulation as illustrated in Figure 3. The central blood compartments (Arterial blood and venous blood) are further divided into blood cells and plasma [9]. Solid organs are further divided into plasma, blood cell, interstitial and intracellular spaces. As cisplatin is intravenously (IV) injected into a vein, it subsequently enters each vascular organ compartment by arterial blood flow and leaves by venous blood flow in the systemic circulation. It is noted that using the PBPK modelling technique, the PK of a drug can also be predicted for individuals with particular organ impairments. For example, for a patient with a renal impairment, the metabolism of the drug in kidney can easily be manipulated. The basic principle is that the PK of cisplatin is studied and predicted by measuring the plasma drug concentration of the whole body that is accessed with different algorithms for particular organ compartments interconnected by the physiological blood flow.
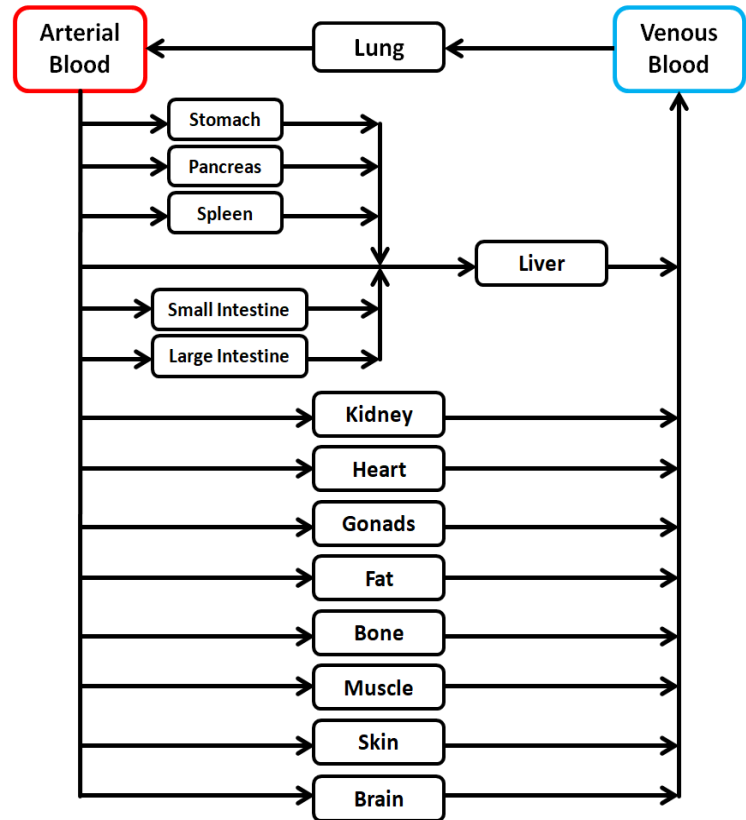
Figure 3: Scheme for the pharmacokinetic 17 compartment model

Chapter 2 Research Design and PBPK Modelling Workflow

2.1 Research Design

In order to construct a PBPK model, experimentally obtained PK datasets of cisplatin for both rats and humans must first be collected as they are of primary importance in optimizing the parameters, validating the PBPK models, and most of all in ensuring that sufficient data are available to create a model. The details of the parameters such as to how they can be selected are addressed in Chapter 3. Physicochemical data such as lipophilicity, molecular weight, and the ADME parameters (from drug-organism interaction) are also collected from the experimental data reported in the literature.

In this thesis, the pharmacokinetics (PK) of cisplatin is analyzed by reproducing a number of observed PK data which describe the drug kinetics as the drug mean concentration in plasma over time profile. The experimentally obtained physicochemical data of cisplatin and applicable anatomical and physiological data that are stored in the PK-Sim platform are fused with defined drug administration protocols to construct an initial PBPK model. While the simulated PK profiles from the model are fitted with the *in-vivo* PK data, the parameters are simultaneously optimized. It should be noted that despite the presence of several reported values of lipophilicity of cisplatin, the most uncertain physicochemical parameter, lipophilicity, also has to be optimized because it is a very sensitive parameter in PBPK simulations.

2.2 PBPK Modelling Workflow

In model development, an initial PBPK model is constructed based on observed PK datasets for rats following cisplatin administration using various methods: different doses of Intraperitoneal (IP) bolus and Intravenous (IV) bolus. Through numerous simulations, parameters are optimized numerically by fitting the PBPK model to the experimental cisplatin PK profiles or cisplatin mean concentration in plasma over time profiles. This numerical optimization is based on a Monte-Carlo algorithm and it will be described in Chapter 4.

In the next step for model evaluation, the developed model is evaluated by comparing the simulated PK profile with other observed PK data with different administration protocols. As will be addressed in detail in the following sections, a successful PBPK model must obtain the consistency of PK predictions against any change in administration protocol, though discrepancies between simulated and experimental data inevitably occur. In other words, a good PBPK model would consistently produce a PK profile in good agreement with observed data for any administration route or dosing regimen. In this thesis, the PBPK model constructed based on observed PK datasets with cisplatin administrations of IP bolus and IV bolus is evaluated by simulating the PK profiles of IV bolus and IV infusion administrations with different doses and comparing them with the corresponding observed PK datasets. With the use of the PK-Sim, the consistency of the PBPK model can still be obtained even against systemic changes like ontogeny variability [11]. Lastly, the PBPK model constructed and evaluated based solely on observed PK datasets for rats is translated into a human model and the validity of the interspecies extrapolation is assessed. As will be discussed in more detail in Chapter 5, the parameters that have been optimized from the rat model are directly applied to the human model and then the simulated PK profile is compared with observed PK datasets for humans. Additionally, the drug and enzyme kinetics that make it possible to directly transfer the optimized values to different models will be demonstrated in Chapter 4.

The PBPK modelling workflow is summarized in Figure 4, which illustrates how reliable pharmacokinetics (PK) predictions of cisplatin can be made theoretically. This workflow is universal and can be applied to further investigations of other scenarios of interest. For instance, the PK prediction of a different drug may be achieved by following this workflow description. However, during the modelling process, different parameters will be utilized depending on the absorption, distribution, metabolism, and excretion (ADME) details of the specific drug in an organism.
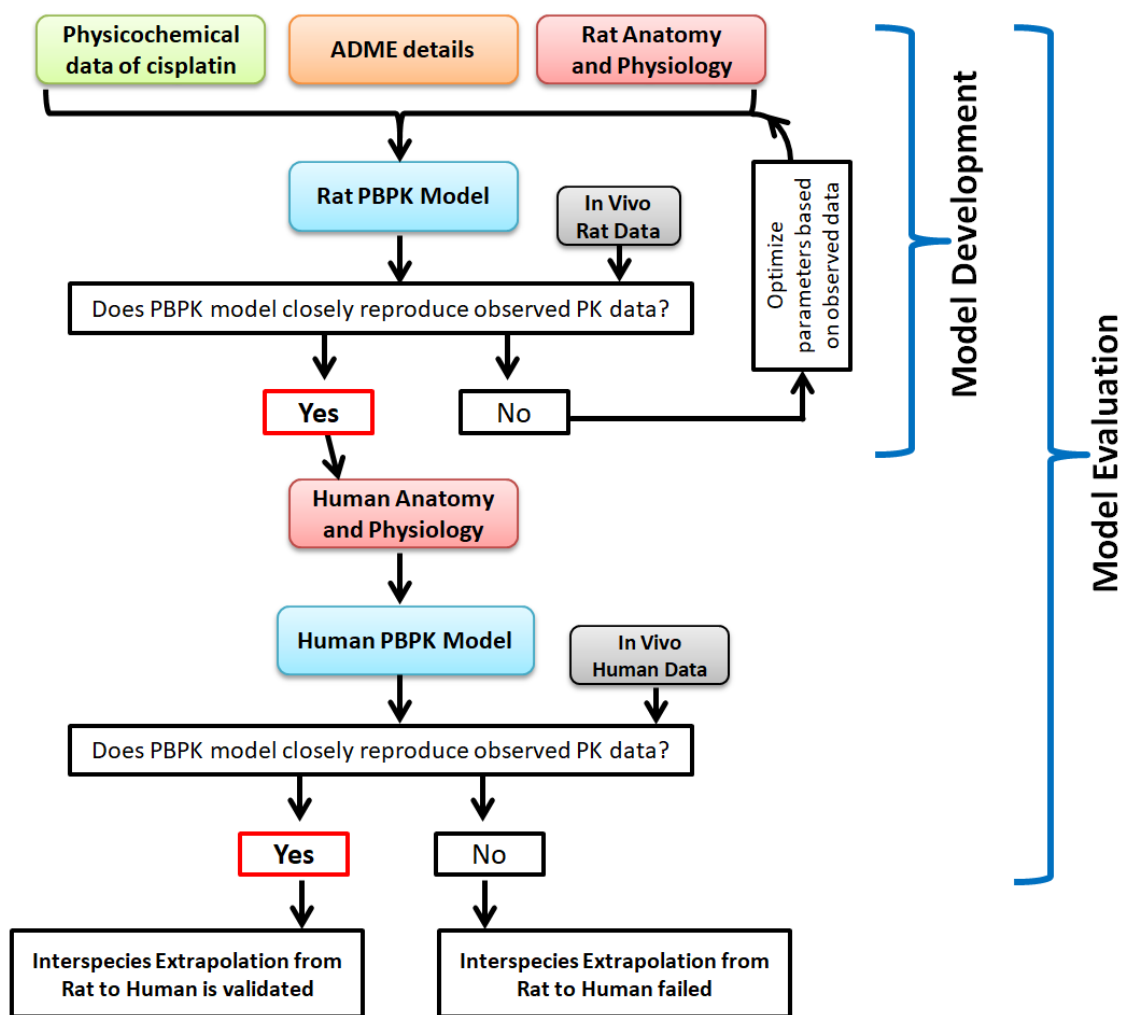
Figure 4: PBPK modelling workflow for cisplatin

9

Chapter 3 Required Data and Assumptions Prior to the PBPK Modelling

3.1 Requirements Prior to the PBPK Modelling

For the PBPK model of one drug to be generated, the drug's physicochemical data and information on drug absorption, distribution, metabolism, and excretion (ADME) are necessary. The physicochemical data should include the drug's molecular weight, number of halogens in the molecule (if applicable), acidity, and lipophilicity. As previously stated, lipophilicity, a very sensitive parameter in PK simulations, is the only physicochemical parameter that is to be optimized while other physicochemical data are fixed in the modelling process. The ADME information includes many pharmacokinetic details such as metabolizing enzymes, fraction unbound, protein transporters, renal clearance rate, inhibition and induction (if applicable), etc. The more are the ADME details, the more realistic and reliable is the constructed model, which better reflects the real pharmacokinetics (PK) of the drug in an organism. Sometimes, there may not be sufficient ADME information available for some drugs, including cisplatin, which makes the PBPK modelling challenging. In such a case, the PBPK modelling essentially requires reasonable assumptions which must be supported by solid justification.

The data required for the PBPK modelling can be split into three groups: physicochemical data for the drug, ADME data, and PK datasets. The first two groups are used in constructing an initial PBPK model with proposed parameters, while the last group is used in optimizing and validating the parameters in both model development and model evaluation processes. This chapter describes the first two data groups for cisplatin, and the required assumptions that lead to the determination of the parameters.

3.2 Physicochemical Properties of Cisplatin and Available ADME Data

As previously stated, the drug's physicochemical data and absorption, distribution, metabolism, and excretion (ADME) data are fundamental elements in developing the PBPK model. During the optimization process, the organ specific tissue-to-plasma partition coefficients which account for the extent of drug distribution over the body are simultaneously determined from many physicochemical parameters and the ADME parameters such as fraction unbound, and fraction excreted to urine. Physicochemical and ADME data of cisplatin that are used in developing the PBPK model, either as input parameters or as references in the optimizing process, are listed in the table below. Two values for the lipophilicity exist in the literature. It should be emphasized that although lipophilicity is a physicochemical property of the drug, it is to be optimized in the range between the two reported values because it is a very sensitive parameter in the PBPK simulation.

Table 1: Physicochemical and ADME properties of cisplatin

	Cisplatin
Molecular weight (g/mol)	300.046 [12]
pKa	5.06 (Strong basic) [13]
Lipophilicity, LogP	-2.19 [14], 0.041 [13] To be optimized in the model
Fraction unbound Rat Human	 62.5%~4.4% (15mins~3hr) [15] 93.51%~8.98% (30mins~3hr) [16]
Fraction excreted unchanged to urine Rat Human	 3.46%~33.8% (10mins~1.5hr) [17] 15.3% at 3hr & 22.5% at 5.5hr [18]

3.3 Metabolism of Cisplatin

3.3.1 Experimental Observations

Formation of Cisplatin-Metabolite and Cisplatin-Albumin/Intracellular protein/DNA Complex

Cisplatin is not a substrate of active metabolic enzyme such as a member of cytochrome P450 which is responsible for metabolizing most drugs during the phase I reaction. Early on when cisplatin had just been approved by the FDA, it was conventionally known that once cisplatin is administered into an organism, the drug is converted into other compounds [19]. However, with the advent of chemical separation techniques, it is currently believed that cisplatin gets metabolized to form metabolites. Following a chromatographic procedure, Daley-Yates and McBrien successfully found 6 different cisplatin-metabolites [15]. Additionally, intact cisplatin binds to albumin, intracellular protein or DNA and recent studies have experimentally shown that the product of metabolized cisplatin, cisplatin-metabolite, also binds to the albumin, or intracellular protein [20].

Anticancer Effect and Nephrotoxicity from Cisplatin-Metabolite and from Cisplatin-Albumin / Intracellular protein / DNA complex

The reaction of forming the cisplatin-albumin / intracellular protein / DNA complex is an irreversible process and the complex is commonly believed to be therapeutically inactive and it does not cause any significant nephrotoxicity [20], [21], [22], [23]. Therefore, the formation of cisplatin-albumin / intracellular protein / DNA complex is considered as a permanent inactivation of cisplatin in the anticancer treatment.

Cytotoxicity and nephrotoxicity of cisplatin-metabolites have been ongoing subjects of investigation. Alden and Repta provided experimental evidence where adding the methionine in cisplatin treatment enhanced the nephrotoxicity, arguing that one of the most abundant cisplatin-metabolites, cisplatin-methionine complex, contributes to the nephrotoxicity [24]. Cisplatin-GSH

complex, the most abundant cisplatin-metabolite, was also found to cause serious nephrotoxicity from the anticancer treatment [25]. On the other hand, several groups have reported that cisplatin-methionine does not show any significant anticancer activity [15] or nephrotoxicity [15], [26], [27]. One study showed that the parent drug, cisplatin, is the most toxic species among all other cisplatin-metabolites and therefore the cytotoxicity and nephrotoxicity decrease as more cisplatin-metabolites are formed [28]. Another group experimentally demonstrated that in plasma cisplatin-metabolites are less toxic than cisplatin and are not significantly contributing to the nephrotoxicity [20]. As will be addressed in followings, cisplatin-metabolites are assumed to cause no anticancer effect in this thesis.

Hydrolysis of Cisplatin Before Being Metabolized or Binding to Albumin, intracellular protein or DNA

After cisplatin administration, it is commonly believed that most cisplatin compounds undergo hydrolysis in biological fluids and they are transformed into hydrated cisplatin species [29], [30]. This is due to the replacement of chloride ions with water or hydroxide ions arising from the low concentration of the chloride ions in the surrounding and the tendency of the system to reach quasi-equilibrium between the unchanged cisplatin and its hydrated species {cis-[Pt(NH$_3$)$_2$ClOH] cis-[Pt(NH3)$_2$(OH)$_2$], cis-[Pt(NH$_3$)$_2$Cl(H$_2$O)], cis-[Pt(NH3)$_2$(H$_2$O)$_2$], cis-[Pt(NH$_3$)$_2$(OH)(H$_2$O)]} [31]. In the quasi-equilibrium state, any residual hydrated species posses the same pharmacokinetics (PK) properties of unchanged cisplatin. This hydration reaction is the rate-limiting step [32], [33], so it is believed that the hydrated species which are more reactive and unstable are transient (or intermediates) before binding to albumin, methionine, or glutathione in plasma. Binding of the hydrated species to two neighboring guanine, G bases in DNA, however, may not likely occur as it was experimentally shown that this binding process is very difficult under normal physiological condition [34]. As stated in Chapter 1, binding of cisplatin to DNA is preferentially promoted by dissociative electron transfer (DET) reaction of cisplatin where cisplatin is attracted by G base which is the most nucleophilic among the four DNA bases [6]. It needs to be emphasized that the DET reaction occurs much faster than hydrolysis process and the displacement of chloride ions from cisplatin may be dominantly initiated by the DET reaction for other cisplatin bindings as well.

Formation of Major Cisplatin-Metabolites via DET reaction

In the order of abundance (or preferential binding) in an organism, cisplatin targets peptides (predominantly Glutathione (GSH)), amino acids (mostly methionine and cysteine), albumin and DNA. Cisplatin-GSH complex constitutes approximately 60% of cisplatin-metabolites [35] and it is therefore considered as a major cisplatin-metabolite. The essential and semi-essential amino acids methionine and cysteine respectively are the next most abundant targets for cisplatin [32], [33]. It was experimentally found that cisplatin strongly binds to methionine and cysteine [36], [37].

The preferential binding of cisplatin which produces many cisplatin-metabolites is believed to be due to the high cisplatin affinity to nucleophiles or sulfhydryl groups of the addressed peptides and amino acids [37]. The sulfhydryl groups, having high nucleophilicity, attract cisplatin to induce nucleophilic displacement of the chloride ions via dissociative electron transfer (DET) reaction to form more electrically stable cisplatin-metabolites. The DET reaction is demonstrated in Equation 1.

The anticancer effect arises when cisplatin binds to DNA after displacement of chloride ions. Once cisplatin-metabolite such as complex of cisplatin-GSH, -methionine, or -cysteine is formed, the complex is electrically stable enough so it does not require electron transfer from DNA guanine, G base. In other words, the cisplatin-metabolite will not bind to DNA and therefore, will cause no anticancer effect. It will either bind to albumin, intracellular protein, or be excreted through urine as will be detailed in later section. In addition, it has been reported that the GSH level is associated with resistance of cancer cells to cisplatin [38].

As will be explained in more details in the next section, the mean molecular weight of cisplatin-metabolites needs to be calculated because cisplatin-metabolite as well as the parent drug, cisplatin must be included as a fundamental component in the PBPK model. The calculation and steps to get the mean molecular weight of cisplatin-metabolites will be demonstrated. Table 2 shows the molecular weights of cisplatin, chloride ion, glutathione, methionine, and cysteine that are used to calculate the molecular weights of the 3 major cisplatin-metabolite complexes which are also shown.

14

Table 2: Molecular weights of cisplatin, chlorine ion, glutathione, methionine, cysteine, and the 3 major cisplatin-metabolites

	Cisplatin	Cl-	Glutathione (GSH)	Methionine	Cysteine
MW (g/mol)	300.046 [12]	35.45 [39]	307.33 [40]	149.208 [41]	121.16 [42]
MW of the complex form (MW of 2Cl is subtracted)			**536.4695**	**378.356**	**350.306**

3.3.2 Necessary Assumptions

As briefly described in section 3.1, in the PBPK model development process, making assumptions on ADME information is sometimes necessary, especially when drug's metabolic details are not sufficiently established. For instance, cisplatin is not metabolized by commonly known enzymes but rather establishing quasi-equilibrium or electron transfer is found to promote the metabolism of cisplatin. In this section, necessary assumptions on ADME details are described and terms that are frequently used from here on are defined.

Cisplatin-metabolite is subject to either bind to albumin, intracellular protein or be excreted out of the organism by having relatively low molecular weight and mobility in plasma, cell or interstitial space. Therefore, it is often called as a *mobile metabolite*. The mobile metabolite is any metabolized form of cisplatin that is not bound to albumin, intracellular protein, or DNA. On the other hand, by having relatively high molecular weight, cisplatin-albumin / intracellular protein / DNA complex is assumed not to be appreciably cleared or redistributed throughout the time course of pharmacokinetic (PK) analysis in animal studies (up to 4 hours) and in human studies (up to 6 hours). It is assumed to be fixed and accumulated in an organism and therefore, it is called as a *fixed metabolite*. The albumin, intracellular protein or DNA-unbound platinum species including intact cisplatin and mobile metabolite are defined as *ultrafilterable platinum*.

Based on the experimental evidence for the metabolism of cisplatin, following statements can be summarized. Cisplatin is metabolized to form a mobile metabolite, while a fixed metabolite is irreversibly formed from binding of either intact cisplatin or mobile metabolite to the albumin, intracellular protein or DNA. To be more specific for the formation of fixed metabolite, intact cisplatin binds to all albumin, intracellular protein, and DNA but mobile metabolite binds to only albumin, and intracellular protein. Therefore, only intact cisplatin is responsible for therapeutic effect due to its capacity to bind to DNA for cancer cell death. These formations can occur through the transient stage, the hydrolysis of cisplatin, but they can also be initiated immediately after cisplatin administration without going through the hydrolysis. In particular, binding of cisplatin to DNA is initiated immediately through the dissociative electron

transfer (DET) reaction. The ultrafilterable platinum, including the intact cisplatin and the mobile metabolite, is albumin, intracellular protein or DNA-unbound platinum species. Additionally, the biliary clearance of cisplatin is negligibly small [43], so in the course of the PBPK modelling in this thesis, only urinary excretion is considered as a route of drug excretion.

The metabolism of cisplatin based on the experimental evidence is illustrated in Figure 5 below. Cisplatin is metabolized to form the mobile metabolites in both plasma space and cell space and the corresponding metabolizing rates are respectively represented by Kmet_Plasma and Kmet_Cell. Cisplatin may bind to a peptide or an amino acid, forming the mobile metabolite (solid rectangle in blue in Figure 5). The irreversible formations of fixed metabolite from intact cisplatin in plasma space and in cell space are handled by binding rates of Kbind1 (Albumin), Kbind1 (Int. Protein) and Kbind1 (DNA). Additional binding rates for the irreversible formation of fixed metabolite from mobile metabolite in plasma space and in cell space are represented by Kbind2 (Albumin) and Kbind2 (Int. Protein) respectively. It is noted that only Kbind1 (DNA) is responsible for the actual antitumor activity. Kp represents partition rate of low molecular weight species (excluding the fixed metabolite) through biological spaces.
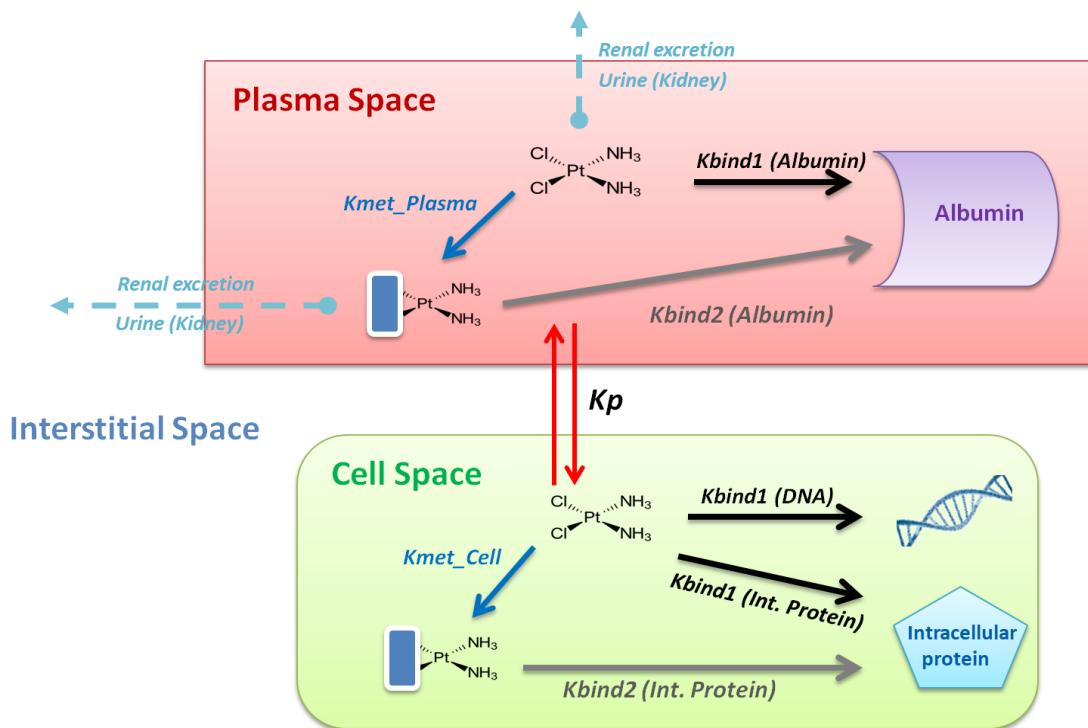
Figure 5: Metabolism of cisplatin based on experimental evidences

To minimize the complexity of constructing the PBPK model while concisely preserving the purpose of the thesis, a number of assumptions have been made. It should be emphasized that the new metabolizing and binding rates or parameters that will be presented, are chosen only for the purpose of analyzing the pharmacokinetics (PK) of cisplatin.

The assumptions on cisplatin metabolism are the following: *Kbind1* represents the rates of irreversible binding of the intact cisplatin to albumin in plasma and to intracellular protein, and DNA in cells. *Kbind2* represents the rates of irreversible binding of the mobile metabolite to albumin in plasma, and to intracellular protein in cells. The two metabolizing rates, Kmet_Plasma and Kmet_Cell that are occurring in both plasma space and cell space are characterized by *Kmet*. The K_m of the urinary excretion is assumed and set to be the same for the mobile metabolite as for the intact cisplatin, where K_m, the Michaelis-Menten constant, is a concentration of a substrate (unchanged cisplatin or mobile metabolite) allowing the renal system to achieve half the maximum rate of urinary excretion in this context.

Based on these assumptions, the PBPK model must be constructed such that the mobile metabolite irreversibly binds to albumin or intracellular protein and also it is excreted through urine. To do so, virtual mobile metabolite, which physicochemically represents the mean mobile metabolite, needs to be created as the intact cisplatin is created. The three major mobile metabolites that are formed most abundantly are produced from cisplatin interaction with glutathione (GSH), methionine, and cysteine. By subtracting the molecular weight of 2 chlorine ions from the molecular weight of intact cisplatin and adding it to the molecular weight of the binding species, the molecular weight of the corresponding mobile metabolite can be estimated, and the molecular weights of the three are listed in Table 2. As stated earlier, approximately 60% of the mobile metabolites are cisplatin-GSH complex [35], so it can be expected that the other 40% are mostly constituted of methionine and cysteine metabolites. In this thesis, it is assumed that the other 40% are equally produced by the two mobile metabolites as no other data regarding the mobile metabolite composition was found. The molecular weight of the mean mobile metabolite is therefore calculated to be 467.6 g/mol.

3.4 Parameters

Parameters are to be mathematically optimized based on observed rat PK data using a Monte Carlo algorithm during the PBPK model development process. Seven parameters are used for the purpose of the thesis. Three of them (Kbind1, Kbind2, and Kmet) are from cisplatin metabolic processes as described in previous section. The remaining parameters are two lipophilicity values and two TSmax values one each for intact cisplatin and mobile metabolite. TSmax represents the maximum tubular secretion rate. As will be described in more details in Chapter 4, the renal clearance is set to be handled by active passive process, glomerular filtration, and passive process, tubular secretion. The seven parameters are summarized in the table below.

Table 3: Seven parameters to be optimized

	Intact cisplatin		Mobile metabolite
Metabolic process	Kbind1	Kmet	Kbind2
Renal clearance	TSmax (Intact cisplatin)		TSmax (Mobile metabolite)
Sensitive physicochemical parameter	Lipophilicity (Intact cisplatin)		Lipophilicity (Mobile metabolite)

Chapter 4 Model Development

4.1 Introduction

The PBPK model is mechanistic in nature as it integrates the physicochemical properties of a drug with the anatomical and physiological system to describe drug kinetics while investigating the absorption, distribution, metabolism, and excretion (ADME) information such as tissue-to-plasma partition coefficients and intrinsic clearance.

Owing to the mechanistic pharmacokinetics (PK) modelling approach in each organ compartment, the detailed quantitative assessment of cisplatin and its tissue and plasma disposition can be determined. During the parameter optimization process in model development, the organ specific tissue-to-plasma partition coefficients which account for the extent of drug distribution over the body are simultaneously determined from the physicochemical properties of the drug and the drug interactions with anatomy and physiology based on the tissue composition.

This chapter describes the development of a rat model which will be evaluated and translated into a human model for validation in Chapter 5. The initial PBPK model is constructed solely based on the physicochemical data of cisplatin, the anatomy and physiology of rats, and the assumptions made on the ADME details. This model will be fitted to the mean plasma concentration over time profiles of six observed PK datasets for rats while the parameters are optimized. Further model evaluation will be presented in Chapter 5.

Enzyme Kinetics in PK Analysis of Cisplatin

The first order reaction rate constants, Kbind1, Kbind2 and Kmet that have a characteristic of an intrinsic clearance must be obtained to study and predict the PK of cisplatin because they need to be uniquely defined or optimized to work globally under different drug concentrations. In other words, one particular optimized value of the rate constant should be used to simulate various PK profiles according to the drug concentration that is administered. The relationship of the first order reaction rate constant, K with the drug concentration dependent metabolizing, or binding rate (M or B) is shown in equation below.

$$M \quad or \quad B \quad = \quad K * [Drug]^1 \tag{2}$$

Therefore, in the building block setting, the three metabolic clearance rates are to be set as intrinsic clearances which are under the so called linear first order kinetics to avoid enzyme saturation as will be demonstrated in section 4.2.2.

As for renal clearance, the Michaelis-Menten constant, K_m, defined as the concentration of a substrate (intact cisplatin or mobile metabolite) at half the maximum rate, V_{max} of the drug elimination in the renal system should be set at a high value in order to achieve the linear first order kinetics. The actual ADME setting including the renal clearance of K_m is presented in the next section. The rate of metabolism, M, and the clearance rate, CL, are defined respectively as:

$$M = \frac{Vmax * C}{Km + C} \quad , \quad CL = \frac{M}{C} \tag{3}$$

where V_{max} is the maximum rate of metabolism and C is drug concentration. If K_m is much larger than C, Equation 3 becomes:

$$M \approx \frac{Vmax * C}{Km} \quad , \quad CL = \frac{Vmax}{Km} \tag{4}$$

and the drug concentration independence and the linear first order kinetics condition are fulfilled in the renal system as well.

Accordingly, both metabolic and renal clearances in the PBPK model are to be set to follow the linear first order kinetics and this set-up is to be validated by observing the 'real' linearity of cisplatin kinetics during the model evaluation process.

4.2 Method

4.2.1 PK Data Acquisition

Six different mean plasma concentration over time profiles from five different cisplatin PK study groups have been chosen for the optimization process [15], [17], [20], [44], [45]. In the digitizing process, the web-browser-based digitizing software WebPlotDigitizer were used to extract numerical PK data from the plots [10]. With the molecular weights of cisplatin (300.046 g/mol [12]) and platinum (195.08 g/mol [46]), the species concentrations in plasma have been converted into molar masses because it allows to avoid calculating the mass concentration (e.g ug/mL) for each molecular species such as concentration of cisplatin or platinum.

4.2.2 Basic Building Block Setting

Compounds: Cisplatin and Mobile Metabolite

In creating cisplatin as a virtual compound in the PK-Sim platform, the physicochemical properties listed in Table 1 were used. As previously mentioned, lipophilicity is a very sensitive physicochemical parameter in the PK simulation. For example, a slight increase in lipophilicity will significantly increase the tissue-to-plasma coefficient and thus increase the volume of distribution. Consequently, the drug will be eliminated at a slower rate and this will be indicated by less steep slope in the PK simulation. Therefore, the lipophilicity is treated as a parameter and is expected to be optimized to a value between the two experimentally observed values.

Based on the assumptions presented in Chapter 3, the ADME setting of cisplatin was made as follows. Cisplatin is metabolically cleared by Kbind1 (binding to albumin, intracellular protein, or DNA) and by Kmet (being metabolized). When cisplatin is cleared by Kbind1, the resulting product, fixed metabolite gets accumulated. When cisplatin is cleared by Kmet, the mobile metabolite is formed and this is to be further processed as will be addressed later in this section. Cisplatin is also renally cleared by tubular secretion (Km set as 1000 μmol/l), and Glomerular filtration (GFR fraction set as 1).

It is noted that the first order process was chosen for all three Kbind1, Kbind2, and Kmet to avoid enzyme saturation. The enzyme saturation in this context represents a situation where metabolizing or binding rate (different from the first order reaction rate constant) stops increasing at certain cisplatin concentration when cisplatin concentration is increasing. A high number of K_m, 1000 μmol/l was chosen for the tubular secretion to achieve the linear first order kinetics under the Michaelis-Menten kinetics due to the reason addressed above. The tubular secretion of cisplatin is to be investigated by optimizing TSmax during the model development process. Given that tubular secretion occurs, it is often preferred to have the glomerular filtration rate, GFR at its maximum, GFRmax which will also contribute to the renal clearance process. To account for the GFRmax, defined below, GFR was set as 1.

$$GFRmax \quad = \quad GFR * (Fraction\ Unbound) \quad\quad\quad (5)$$

The mobile metabolite must also be included as a virtual compound in order to account for its elimination during the pharmacokinetics (PK) process. On the other hand, the fixed metabolite is assumed to be accumulated in the time course of pharmacokinetic (PK) analysis so it was not necessary to create one for the fixed metabolite. The ADME setting of the mobile metabolite was made the same as for cisplatin, except that it is missing the Kbind1 since Kbind1 is a metabolic clearance rate only for the intact cisplatin to be metabolized whereas mobile metabolite is the final product after the Kbind1 action.

Individuals: Rats with Various Weights

Virtual rats were separately created according to the anatomical data of rats presented in different studies. Weight is the only variable among virtual rats. The metabolic expression of the rat was then set to link to the three clearances (Kbind1, Kbind2, and Kmet) of cisplatin. It is noted that the renal clearances are already linked by default.

Formulations and Administration Protocols

The formulation type was set as 'dissolved' as cisplatin is always injected intravenously (IV) as a dissolved solution. Other formulation types such as 'weibull distribution' would require a drug dissolution time or lag time to be entered for an orally taken drug, such as tablet. For the administration protocols, different doses and administration types were separately assigned according to the protocols that the pharmacokinetics (PK) studies used. In this thesis, only an administration of a single dosing interval is used. However, developing cisplatin PBPK model of multiple dosing intervals is certainly practicable and may be pursued in a future project. The administration protocols of the six different PK profiles that have been used to optimize the parameters are shown in the table below.

Table 4: Administration protocols used by cisplatin PK groups

	Administered Drug	Administration type	Dose (mg/kg)
Hanada et al. [20]	Cisplatin	Intravenous (IV) bolus	5
Hanada et al. [20]	Mobile metabolite	Intravenous (IV) bolus	8.389
Yates and Mcbrien [15]	Cisplatin	Intraperitoneal (IP) bolus	15
Nagai et al. [17]	Cisplatin	Intravenous (IV) bolus	5
Fukushima et al. [44]	Cisplatin	Intravenous (IV) bolus	5
Okada et al. [45]	Cisplatin	Intravenous (IV) bolus	5

It is noted that the rat PK of mobile metabolite has been studied by Hanada et al. [20] and it is of particular importance in investigating the mobile metabolite kinetics associated with the fixed metabolite accumulation in the body. The elimination of the administered mobile metabolite and the resulting production of the fixed metabolite over time are well studied by the group. Therefore, by adopting this PK profile data of the mobile metabolite as one of the six optimizing components (six observed PK datasets), the rate of irreversible binding of the mobile metabolite to produce the fixed metabolite, Kbind2 can be determined. For the administered mobile metabolite dose, Hanada et al. used 'platinum concentration' in the plasma (3.5 mg (pt) / kg) while other PK studies with cisplatin administration used 'cisplatin concentration' in the plasma (e.g 5 mg (cisplatin) / kg). The mobile metabolite administration dose must be converted to be expressed as 'mobile metabolite concentration' which is essentially required to be entered in the PBPK model development process. The molecular weights of platinum and mobile metabolite (calculated in section 3.3.2) have been used to convert it as following:

$$3.5 \text{ mg (pt) / kg} * \frac{467.6 \text{ g/mol} \quad \text{(mobile metabolite MW)}}{195.08 \text{ g/mol} \quad \text{(platinum MW)}} = 8.389 \text{ mg (mobile metabolite) / kg}$$

(6)

4.2.3 Simulation Setup

The term simulation can be ambiguous to some extent because it can refer to a single species PK simulation or it can also refer to a simulation of one PK study containing many PK simulations. For example, a simulation reproducing an experimental PK study with cisplatin presented by Nagai et al. [17] contains four different PK simulations representing the pharmacokinetics (PK) of intact cisplatin, mobile metabolite, ultrafilterable platinum, and a fraction excreted to urine. Therefore, it needs to be more clearly defined. 'The 6 PK-profile simulations' refers to the six simulations, and each of them contains several PK simulations, developed for the purpose of optimizing the parameters. They are based on the rat PK datasets of six different cisplatin PK studies observed by five different cisplatin PK study groups. A brief description will be included with the result of each simulation. For example, "In the simulation reproducing experimental PK study by Nagai et al. [17], a great agreement can be found between ultrafilterable platinum PK simulation and the corresponding observed PK data"

Additional PK Simulations

As briefly discussed in section 3.3.2, there are species specifically defined for the purpose of this thesis such as mobile metabolite, fixed metabolite and ultrafilterable platinum. The pharmacokinetics (PK) profile of any created compound can be simulated by the PBPK modelling platform, PK-Sim, that is, the PK profiles of cisplatin and mobile metabolite are already formulated to be simulated. As for non-created species such as fixed metabolite and ultrafilterable platinum, however, the corresponding equation is required to be input manually. In the language of Open Systems Pharmacology [9], the formulation modality is referred as 'observers', which allows the desired PK simulation to be generated. The addition of the new PK simulation using the observers has been done through another PBPK modelling platform, MoBi, and the necessary equations for the non-created species that have been added into observers are described in the following.

The fixed metabolite which is assumed to be accumulated in the body is a sum of irreversible binding products from intact cisplatin and mobile metabolite, handled by Kbind1 and Kbind2 respectively. So the fixed metabolite equation has been constructed as:

$$\text{Fixed metabolite} = \text{Kbind1-metabolite} + \text{Kbind2-metabolite} \quad (7)$$

The albumin, intracellular protein, or DNA-unbound platinum species, ultrafilterable platinum, consists of the intact cisplatin and mobile metabolite and therefore, the equation has been constructed as:

$$\text{Ultrafilterable platinum} = \text{cisplatin} + \text{mobile metabolite} \quad (8)$$

Additionally, another equation for fraction unbound was required to be constructed, which by definition accounts for the fraction of therapeutically active species in plasma over the time course of PK analysis. As discussed in Chapter 3, only the parent drug, intact cisplatin which is unbound to albumin, intracellular protein, or DNA is responsible for therapeutic effect due to its capacity to bind to DNA guanine, G base via the dissociative electron transfer (DET) reaction. Therefore, the fraction unbound for cisplatin should be constructed as concentration of unbound cisplatin over sum of concentrations of unbound and bound cisplatin as:

$$\text{Fraction unbound for cisplatin} = \frac{[\text{Unbound cisplatin}]}{[\text{Unbound cisplatin}]+[\text{Bound cisplatin}]} \quad (9)$$

Given that fixed metabolite is produced from both intact cisplatin and mobile metabolite bindings, Equation 9 can be re-written as:

$$\text{Fraction unbound for cisplatin} = \frac{[\text{Unbound Cisplatin}]}{[\text{Unbound Cisplatin}] + [\text{Fixed metabolite from cisplatin binding}]} \quad (10)$$

However, available *in-vivo* data of fraction unbound for cisplatin as defined in Equation 10, could not be found, implying that the fraction unbound can only be simulated without validation. This will be revisited after successfully developing and evaluating the PBPK model when 'actual' cisplatin fraction unbound for cisplatin is predicted in Chapter 5.

Alternatively, fraction unbound data for platinum species could be found and adopted in this thesis for the purpose of developing and evaluating the PBPK model with given PK datasets. Platinum species represents ultrafilterable platinum or any platinum species that is unbound to albumin, intracellular protein, or DNA. Due to the limited data availability of experimentally observed fraction unbound for cisplatin and platinum species, only two PK studies have been found, which presented observed PK profiles of cisplatin species as well as the fraction unbound that are suitable to be adopted in this thesis. For example, fraction unbound data that was observed from rats or humans in the PK analysis time course of less than 6 hours was required in order to have the same experimental settings as for other observed PK datasets adopted for the model development and evaluation processes. The observed data of fraction unbound for platinum species (not cisplatin) could be obtained from the two PK studies; Yates and Mcbrien [15] presented rat pharmacokinetics (PK) of intact cisplatin, ultrafilterable platinum, and fraction unbound for platinum species in the investigation of finding toxicity levels of intact cisplatin and mobile metabolites. This fraction unbound has been used in the PBPK model development process as will be described later in this section. Verschraagen et al. [16] presented human pharmacokinetics (PK) of intact cisplatin, ultrafilterable platinum, and total platinum in the study of evaluating a chemoprotectant candidate against cisplatin-induced side effects. The data of fraction unbound for platinum species could be estimated from given PK data of other cisplatin species as will be shown in Chapter 5 where the PBPK model is validated for its predictive utility for extrapolation from rats to humans. In order to account for the fraction of all albumin, intracellular protein, or DNA-unbound platinum species, a new equation has to be constructed as:

$$\text{Fraction unbound for platinum species} = \frac{[\text{Ultrafilterable platinum}]}{[\text{Ultrafilterable platinum}]+[\text{Fixed metabolite}]} \qquad (11)$$

Fitting PK Fractions to Observed Data

The PK simulation of the fraction unbound has been matched to the platinum species fraction unbound data observed by Yates and Mcbrien [15] to be used in the parameter optimization process along with other pharmacokinetics (PK) simulations.

Another PK fraction that is of paramount importance in the PBPK model development process is 'fraction excreted to urine' as it reflects the renal clearance which contributes to most of the elimination kinetics for the majority of the drugs. As the name implies, it represents the fraction of the administered drug that is excreted to urine as unchanged or intact. The PK simulation of the fraction excreted to urine has been matched to cisplatin fraction excreted to urine data observed by Nagai et al. [17].

4.3 Results

4.3.1 Initial Model Development

The 6 PK-profile simulations have been carefully developed to reproduce the corresponding observed cisplatin PK profiles as closely as possible while parameters are optimized accordingly. All the 6 PK-profile simulations contain intact cisplatin simulation which describes cisplatin pharmacokinetics (PK), the main focus of this thesis. The ultrafilterable platinum simulation is presented in half of the 6 PK-profile simulations among which one requires a calculation to estimate the ultrafilterable platinum PK data. Hanada et al. [20] have presented the PK data for both intact cisplatin and mobile metabolite, so the PK data for ultrafilterable platinum can be estimated by summing the two. As mentioned, the simulations for the fraction unbound and fixed metabolite are presented in the two simulations reproducing experimental PK studies presented by Yates and Mcbrien [15] and Nagai et al. [17] respectively. In order to understand the PK of cisplatin and mobile metabolite with respect to metabolic clearance, it is necessary to observe fixed metabolite production over time. Hanada et al. [20] provided observed data of two PK profiles where the production or accumulation of the fixed metabolite from intact cisplatin administration and from mobile metabolite administration is described. It should be emphasized that the two observed PK profiles play an important role in finding relationships between parameters during the parameter optimizing processes. In particular, the simulated PK profile with mobile metabolite administration provides clear relationship between Kbind2 and renal clearances since there is no Kbind1 or Kmet on action due to absence of the intact cisplatin in the course of the PK analysis. The optimizing processes for determining the parameters by PBPK model fitting to the observed PK profiles is detailed in the following section.

4.3.2 Parameter Optimization

The PBPK model fitting to the observed data has been done by using numerical optimization that is based on a Monte-Carlo algorithm. The Monte-Carlo algorithm provides more accurate results by taking the global minimum of the average error as opposed to taking local minima which are found in the general gradient method. Average error in this context represents an average of the errors from all the parameters that are used. Figure 6 illustrates one
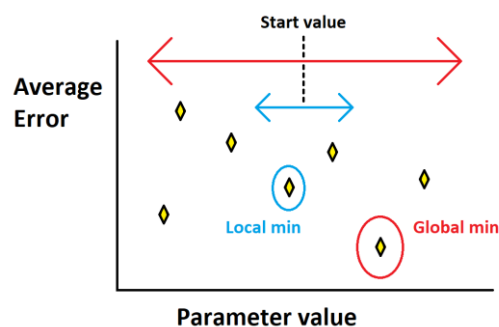
Figure 6: Monte-Carlo method (in red) and gradient method (in blue) in optimization process

parameter being optimized by finding a global minimum value of the average error. In this thesis, this process is applied to all 7 parameters simultaneously. Additionally, in the optimization process, an optimized value of a parameter is said to be a 'unique value' or 'uniquely identifiable value' only if the same value (or a very close value) is obtained from multiple numerical optimizations with different initial values (referred as 'start values' in the platform) of the parameter. In this thesis, this numerical optimization is to be conducted multiple times with different initial values of all the parameters in order to find the unique values.

A total of fifteen simulations, each representing cisplatin species PK, fraction unbound, or fraction excreted to urine in the 6 PK-profile simulations have been matched or coupled with the corresponding observed PK data to conduct the numerical optimization as shown in Table 5. Some of them were coupled with higher weights because their close matches are more significant than others or other matches present more abundantly. For example, all six cisplatin simulations from the 6 PK-study simulations were coupled with the observed data with higher weights because cisplatin pharmacokinetics (PK) is in fact more significant in this study. The two PK fraction matches for fraction unbound and fraction excreted to urine were also weighted higher because each fraction data was provided by one PK study group (e.g fraction unbound data and fraction excreted to urine data were only provided by Yates and Mcbrien [15] and Nagai et al. [17] respectively)

Table 5: Simulation matching with observed data and resulting parameter optimization

	Simulations matched with observed data	Parameters to be optimized
Hanada et al. [20]	Cisplatin PK	Kbind1, Kmet, TSmax (cisplatin), and lipophilicity (cisplatin)
	Mobile metabolite PK	Kmet, Kbind2, TSmax (mobile metabolite), and lipophilicity (mobile metabolite)
	Fixed metabolite PK	Kbind1, Kbind2, lipophilicity (cisplatin), lipophilicity (mobile metabolite)
	Ultrafilterable platinum PK	All 7 parameters
Hanada et al. [20]	Mobile metabolite PK	Kmet, Kbind2, TSmax (mobile metabolite), and lipophilicity (mobile metabolite)
	Fixed metabolite PK	Kbind1, Kbind2, lipophilicity (cisplatin), lipophilicity (mobile metabolite)
Yates and Mcbrien [15]	Cisplatin PK	Kbind1, Kmet, TSmax (cisplatin), and lipophilicity (cisplatin)
	Ultrafilterable platinum PK	All 7 parameters
	Fraction unbound	All 7 parameters
Nagai et al. [17]	Cisplatin PK	Kbind1, Kmet, TSmax (cisplatin), and lipophilicity (cisplatin)
	Mobile metabolite PK	Kmet, Kbind2, TSmax (mobile metabolite), and lipophilicity (mobile metabolite)
	Ultrafilterable platinum PK	All 7 parameters
	Fraction excreted to urine	Kbind1, Kmet, TSmax (cisplatin), and lipophilicity (cisplatin)
Fukushima et al. [44]	Cisplatin PK	Kbind1, Kmet, TSmax (cisplatin), and lipophilicity (cisplatin)
Okada et al. [45]	Cisplatin PK	Kbind1, Kmet, TSmax (cisplatin), and lipophilicity (cisplatin)

Parameter Identification Run Properties

Total Error	3.84
Number of Evaluations	1078
Elapsed Time	28m:55s:240ms
Status	✓ Ran To Completion

Name	Optimal Value	Start Value	Min. Value	Max. Value	
✓ Kbind1	2.84E-3 l/h	1.00E-3 l/h	1.00E-3 l/h	5.00E-3 l/h	
✓ Kbind2	9.74E-4 l/h	1.00E-3 l/h	5.00E-4 l/h	3.00E-3 l/h	
✓ Kmet	0.01 l/h	6.00E-3 l/h	5.00E-3 l/h	0.05 l/h	
✓ TSmax Cisplatin	1.08E-5 µmol/h	1.00 µmol/h	1.00E-5 µmol/h	2.00 µmol/h	
✓ TSmax MobileMetabolite	14.59 µmol/h	1.00 µmol/h	1.00E-5 µmol/h	50.00 µmol/h	
✓ Lipophilicity Cisplatin	-0.43 Log Units	-1.00 Log Units	-4.00 Log Units	0 Log Units	
✓ Lipophilicity MobileMetabolite	-3.76 Log Units	-5.00 Log Units	-6.00 Log Units	0 Log Units	

Parameter Identification Run Properties

Total Error	3.84
Number of Evaluations	1498
Elapsed Time	42m:14s:600ms
Status	✓ Ran To Completion

Name	Optimal Value	Start Value	Min. Value	Max. Value	
✓ Kbind1	2.86E-3 l/h	3.00E-3 l/h	1.00E-3 l/h	5.00E-3 l/h	
✓ Kbind2	9.73E-4 l/h	2.00E-3 l/h	5.00E-4 l/h	3.00E-3 l/h	
✓ Kmet	0.01 l/h	8.00E-3 l/h	5.00E-3 l/h	0.05 l/h	
✓ TSmax Cisplatin	1.94E-5 µmol/h	4.00E-3 µmol/h	1.00E-5 µmol/h	2.00 µmol/h	
✓ TSmax MobileMetabolite	14.61 µmol/h	20.00 µmol/h	1.00E-5 µmol/h	50.00 µmol/h	
✓ Lipophilicity Cisplatin	-0.43 Log Units	-2.00 Log Units	-4.00 Log Units	0 Log Units	
✓ Lipophilicity MobileMetabolite	-3.76 Log Units	-4.00 Log Units	-6.00 Log Units	0 Log Units	

Parameter Identification Run Properties

Total Error	3.84
Number of Evaluations	1848
Elapsed Time	48m:18s:173ms
Status	✓ Ran To Completion

| Name	Optimal Value	Start Value	Min. Value	Max. Value	
✓ Kbind1	2.84E-3 l/h	1.50E-3 l/h	1.00E-3 l/h	5.00E-3 l/h	
✓ Kbind2	9.74E-4 l/h	7.00E-4 l/h	5.00E-4 l/h	3.00E-3 l/h	
✓ Kmet	0.01 l/h	0.02 l/h	5.00E-3 l/h	0.05 l/h	
✓ TSmax Cisplatin	1.47E-5 µmol/h	0.10 µmol/h	1.00E-5 µmol/h	2.00 µmol/h	
✓ TSmax MobileMetabolite	14.61 µmol/h	2.00E-4 µmol/h	1.00E-5 µmol/h	50.00 µmol/h	
✓ Lipophilicity Cisplatin	-0.43 Log Units	-3.50 Log Units	-4.00 Log Units	0 Log Units	
✓ Lipophilicity MobileMetabolite	-3.76 Log Units	-1.00 Log Units	-6.00 Log Units	0 Log Units	

Figure 7: Three numerical optimization results run from different starting values of the parameters (generated by Open systems pharmacology (2019) platform [9])

Three numerical optimizations have been attempted, all run from with initial values of the parameters as shown in Figure 7. On the very right side in the figure, the two diamonds in blue indicate the minimum and maximum values or 'optimizing window', the square in grey indicates the starting value initially set for the parameter to be optimized, and the circle in orange indicate the final optimized values.

Notably, each optimized value for the lipophilicity of cisplatin, lipophilicity of mobile metabolite, and Kmet came out to be exactly the same values from all the three trials. For other parameters, Kbind1, Kbind2, and TSmax for mobile metabolite, very close optimized values could be obtained from the three trials all with less than 0.1% offset. However, the optimized values for the TSmax for cisplatin from the three trials do not appear to be close to each other. In other words, TSmax for cisplatin, which provides kinetic information of the intact cisplatin tubular secretion, was not uniquely identified, and so renal clearance is to be further investigated in a later section. It could be concluded that the parameters, Kbind1, Kbind2, Kmet, TSmax for mobile metabolite, lipophilicity of cisplatin and lipophilicity of mobile metabolite have been uniquely identified which would make the PBPK model closely fit to the observed PK data.

4.3.3 The PK Analysis with PK Simulations with Optimized Parameters

The last set of optimized values in Figure 7 has been chosen to be transferred to the 6 PK-study simulations, although the other sets would work fairly well due to the reasons addressed above. It should be noted that the 6 PK-study simulations are each generated with the same set of optimized values to observe how closely the constructed PBPK model fits the observed PK data, and therefore the optimized parameters are often called as global parameters. These optimized parameters will be evaluated in Chapter 5 as to whether they work globally or not under administration protocols different from what are used in this chapter and moreover, after extrapolating to a human model. In the following, each of the 6 PK-study simulations will be presented with brief descriptions and the PK simulations generated with the optimized values will be compared with observed PK data.
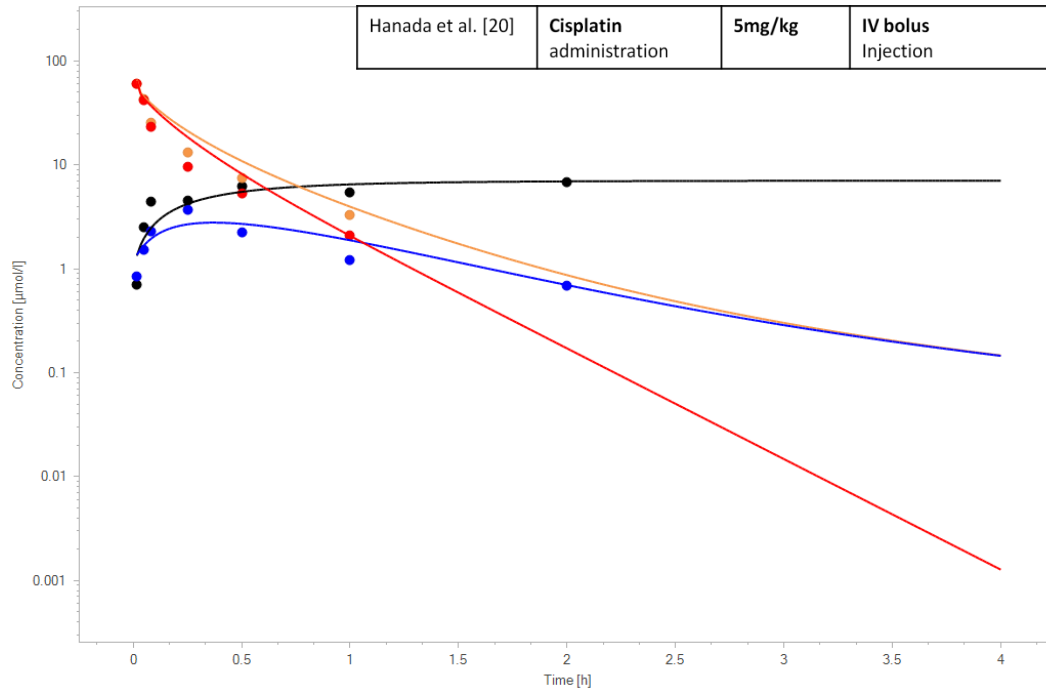
Figure 8: Simulation reproducing experimental PK study by Hanada et al. [20] showing PK simulations (solid lines) of intact cisplatin (in red), ultrafilterable platinum (in orange), mobile metabolite (in blue), and fixed metabolite (in black); solid dots represent experimentally observed values (generated by Open Systems Pharmacology (2019) platform [9])

Figure 8 illustrates PK simulations of intact cisplatin, ultrafilterable platinum, mobile metabolite, and fixed metabolite, reproducing the observed PK data by Hanada et al. [20]. The following descriptions are necessary to understand cisplatin PBPK analysis adopted in this thesis:

➢ Dots represent the observed values and solid lines represent the PK simulations.

➢ Different colors represent different species:

"Intact cisplatin in red", "ultrafilterable platinum in orange", "mobile metabolite in blue", "fixed metabolite in black"

The intact cisplatin simulation and the ultrafilterable platinum simulation predict the concentrations of both species to be a little higher than what are observed in the first hour. The relatively steep decrease in concentration of the intact cisplatin is from the metabolic clearances of all Kbind1, Kmet and renal clearance. The production of fixed metabolite is well reflected by the fixed metabolite simulation. Also, the production of mobile metabolite from the administered cisplatin at the beginning that is handled by Kmet, and the elimination of the mobile metabolite later handled by the balance of Kmet, Kbind2 and renal clearance are in detail described by the mobile metabolite simulation.

35
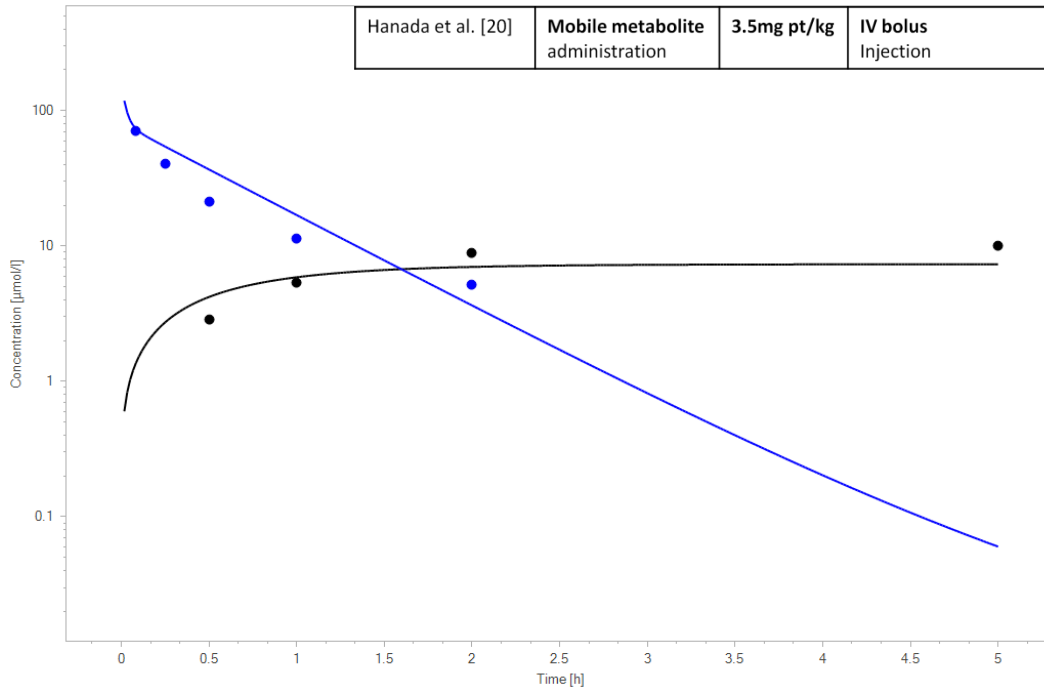
Figure 9: Simulation reproducing experimental PK study by Hanada et al. [20] showing PK simulations (solid lines) of mobile metabolite (in blue), and fixed metabolite (in black); solid dots represent experimentally observed values (generated by Open Systems Pharmacology (2019) platform [9])

Figure 9 illustrates PK simulations of mobile metabolite and fixed metabolite after the mobile metabolite administration, reproducing another observed PK data by Hanada et al. [20]. The significance of this simulation in finding relationships between the metabolic clearances of the parameters (Kbind1, Kbind2, and Kmet) and renal clearance is emphasized in section 4.3.1.

As previously mentioned, there is only Kbind2 as a metabolic clearance process since the mobile metabolite is administered and the intact cisplatin is absent. As a result, the production of the fixed metabolite as shown in Figure 9 is solely made from the mobile metabolites handled by Kbind2 only and is well reflected by the fixed metabolite simulation. The pharmacokinetics (PK) of mobile metabolite is also well described by the mobile metabolite simulation. It is noted that the decrease in the concentration of mobile metabolite is from both Kbind2 and renal clearance, while fixed metabolite is only accumulated because it is neither metabolically nor renally cleared in the time course of the PK analysis.
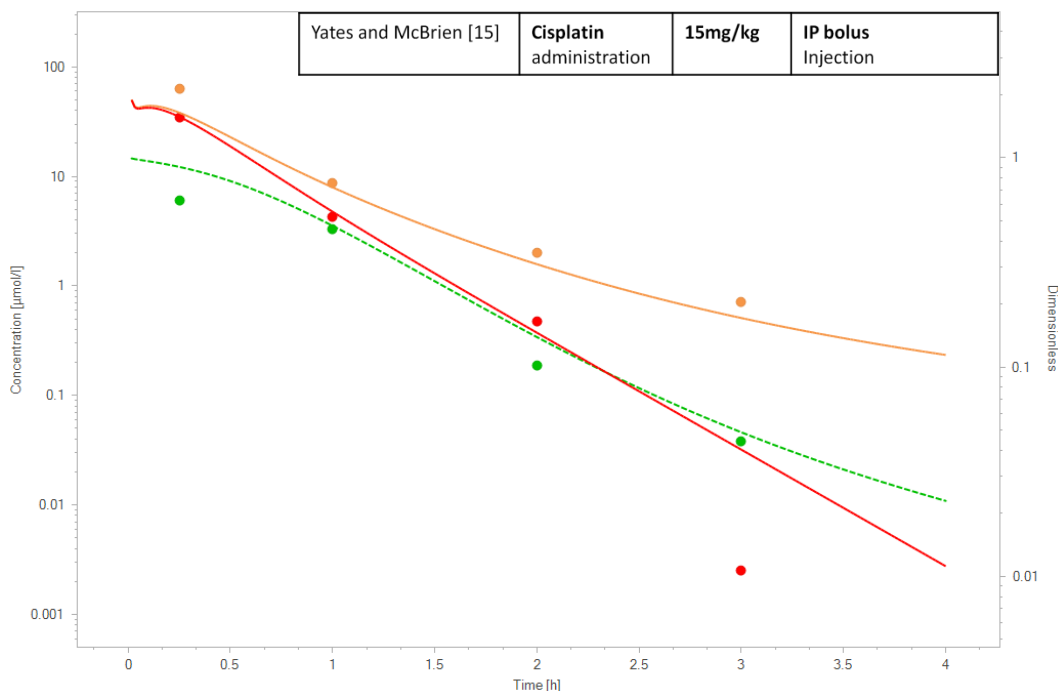
Figure 10: Simulation reproducing experimental PK study by Yates and McBrien [15] showing PK simulations of intact cisplatin (solid line in red), ultrafilterable platinum (solid line in orange), and fraction unbound (dotted line in green); solid dots represent experimentally observed values (generated by Open Systems Pharmacology (2019) platform [9])

Figure 10 illustrates PK simulations of intact cisplatin, ultrafilterable platinum, and fraction unbound reproducing the observed PK data by Yates and Mcbrien [15]. One additional simulation described here is a fraction unbound simulation represented by the dotted line in green.

All simulations generated here appear to adequately reflect the observed PK data except that at an observed time of 15 min, a significant difference is found between concentration of ultrafilterable platinum and that of intact cisplatin by experimental observation whereas only a small difference is predicted by the simulations. According to the observed data, at the start of cisplatin administration, there must be enormous metabolizing activities which cause the split of the intact cisplatin and the ultrafilterable platinum by producing an excess of mobile metabolite. This observation appears to agree with the idea of cisplatin metabolism via dissociative electron transfer (DET) reaction which occurs much faster than hydrolysis under normal physiological condition. Note that an important ADME parameter, fraction unbound, which represents the fraction of albumin, intracellular protein, or DNA-unbound platinum species, or ultrafilterable platinum has also been reproduced in an excellent agreement with the observed data.

37
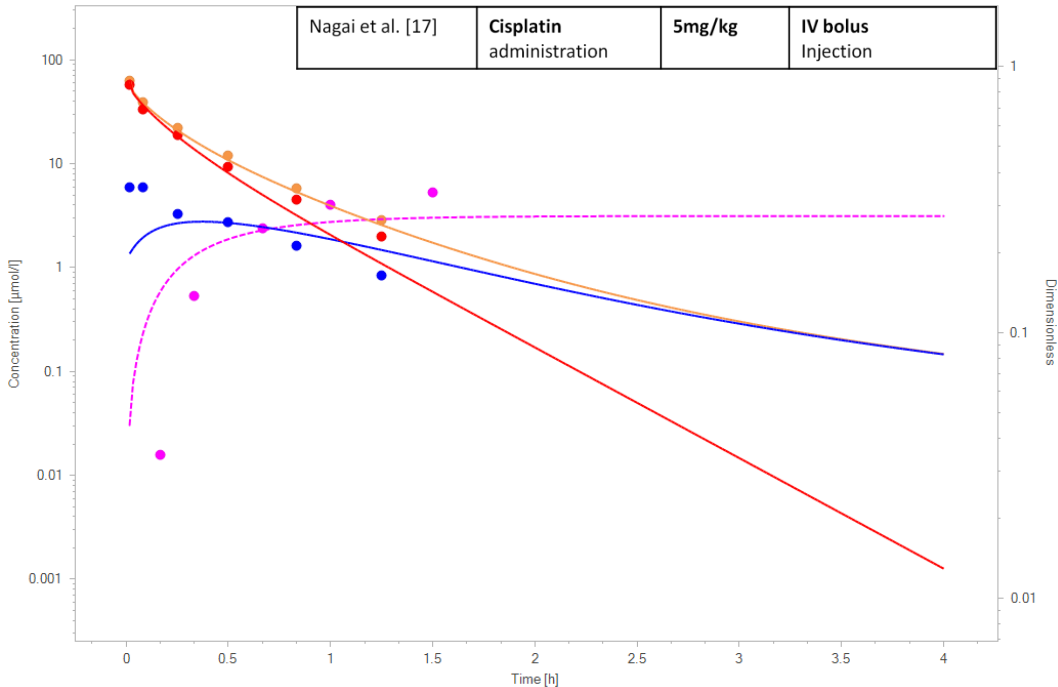
Figure 11: Simulation reproducing experimental PK study by Nagai et al. [17] showing PK simulations of intact cisplatin (solid line in red), ultrafilterable platinum (solid line in orange), mobile metabolite (solid line in blue), and fraction excreted to urine (dotted line in pink); solid dots represent experimentally observed values (generated by Open Systems Pharmacology (2019) platform [9])

Figure 11 illustrates PK simulations of intact cisplatin, ultrafilterable platinum, mobile metabolite, and fraction excreted to urine, reproducing the observed PK data by Nagai et al. [17]. Fraction excreted to urine simulation is represented by the dotted line in pink.

The same administration protocol is followed as in the PK study by Hanada et al. [20] with cisplatin administration, and consequently the same corresponding PK simulations have been generated. For instance, simulations of intact cisplatin, ultrafilterable platinum, and mobile metabolite generated here are the same as those generated in the simulation reproducing experimental PK study by Hanada et al. [20] as shown in Figure 8. Note that by comparing Figures 8 and 11, discrepancies of observed PK data can be easily found between the two PK studies. The observed concentrations of the intact cisplatin and ultrafilterable platinum presented here are appreciably higher than those that are observed by Hanada et al. A considerable difference in the concentration of the mobile metabolite is also found.

The fraction excreted to urine represents the fraction of the intact cisplatin excreted to urine as unchanged and it is particularly important in investigating the renal clearance process. From conducting multiple numerical optimizations with different starting values, it was found that the TSmax for cisplatin is the only parameter that is not uniquely identifiable as demonstrated in section 4.3.2. Additionally, the TSmax for cisplatin was found to be about six orders of magnitude less than TSmax for mobile metabolite from all three attempts of the numerical optimization. Therefore, it was suspected that the intact cisplatin may not be significantly excreted through the tubular secretion process but rather through the glomerular filtration process. So an attempt was made to re-run the Nagai et al. [17] simulation with 0 μmol/h TSmax for cisplatin and the same values of the uniquely found parameters to determine the dependence of TSmax for cisplatin parameter on the fraction excreted to urine simulation. There was no change found in any PK simulation, implying that the intact cisplatin is not excreted through the tubular secretion or the tubular secretion process for cisplatin is negligibly small. The initial hypothesis on the renal clearance was that cisplatin and its metabolites are renally cleared by both the active process, tubular secretion and the passive process, glomerular filtration.

Based on this practice, it could however be concluded that the renal clearance of the intact cisplatin is only processed by the passive process, glomerular filtration, or that the two active and passive processes are both occurring but there is also tubular reabsorption which hinders the tubular secretion. This idea of the glomerular filtration being a dominant renal clearance process and the possible action of the tubular reabsorption were suggested by Yates and McBrien [47]. However, their focus was on the renal clearance of the platinum containing species, the ultrafilterable platinum, rather than on the intact cisplatin or mobile metabolite as investigated in this thesis.

| Fukushima et al. [44] | **Cisplatin** administration | 5mg/kg | **IV bolus** Injection |
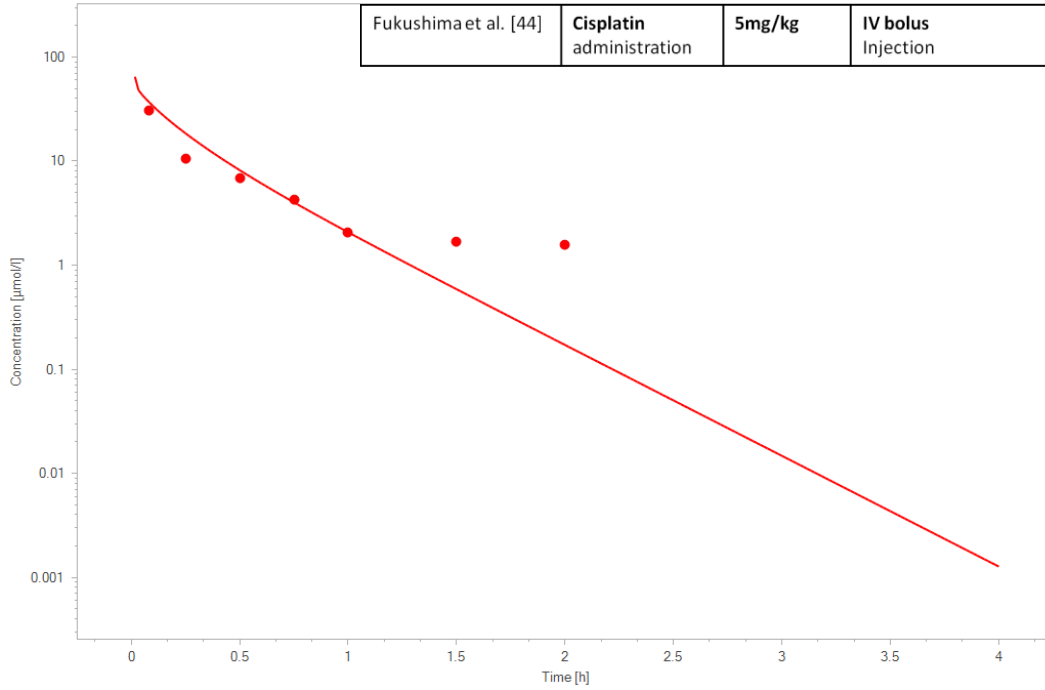
Figure 12: Simulation reproducing experimental PK study by Fukushima et al. [44] showing PK simulation of intact cisplatin (solid line in red); solid dots represent experimentally observed values (generated by Open Systems Pharmacology (2019) platform [9])

| Okada et al. [45] | **Cisplatin** administration | 5mg/kg | **IV bolus** Injection |
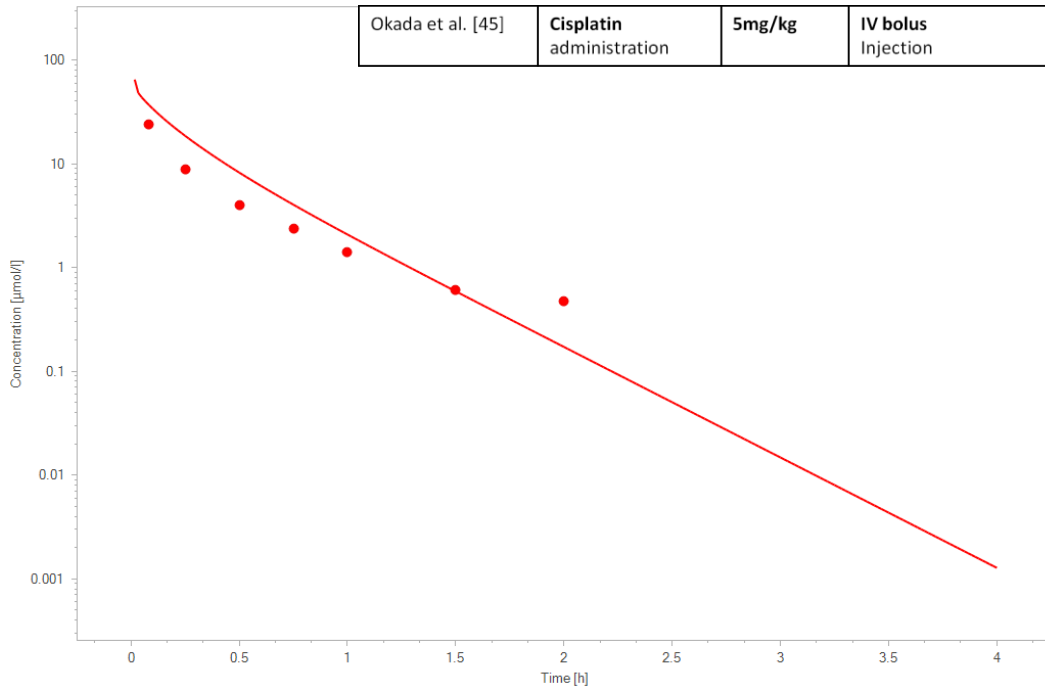
Figure 13: Simulation reproducing experimental PK study by Okada et al. [45] showing PK simulation of intact cisplatin (solid line in red); solid dots represent experimentally observed values (generated by Open Systems Pharmacology (2019) platform [9])

40

Figures 12 and 13 illustrate PK simulations of intact cisplatin reproducing the observed PK data by Fukushima et al. [44] and Okada et al. [45]. It should be noted that only those with observed PK data have been simulated, although other PK profiles can also be predicted by the simulations without the available PK data. For example, as shown in Figure 12, the Fukushima et al. [44] simulation only contains the intact cisplatin simulation because an observed data of only cisplatin PK has been presented by the group, but it is also possible to simulate or predict other PK profiles such as mobile metabolite PK and fraction unbound even if the observed data are not available.

Both PK studies followed the same administration protocol employed in the PK studies by Hanada et al. and Nagai et al. and again the same intact cisplatin simulations could have been generated. In essence, the Figures 8, 11, 12, and 13 show the same simulation for the pharmacokinetics (PK) of the intact cisplatin. In the first hour of the PK analysis, Figure 12 shows a better agreement, but after one hour, Figure 13 shows a better agreement between the simulation and the observed PK data.

4.4 Conclusions

In this chapter, the development processes of the PBPK model for cisplatin have been described, from constructing the initial PBPK model, optimizing and determining the parameters, to analyzing the simulated PK profiles. Most PK simulations appear to have great agreements with the observed PK datasets. The discrepancies among observed PK data arising from different PK study groups even with the same followed administration protocols resulted in inevitable but insignificant discrepancies between the simulations and the observed data. At this point, one should not be confused between this 'check-up' step conducted in the model development and an actual evaluation process in the model evaluation. As the last step in the model development, the constructed PBPK model is checked or tested if the model is acceptable enough to proceed to the model evaluation process or the optimization process will be re-conducted otherwise.

In conclusions, the PBPK model for cisplatin has been successfully developed and therefore, the model is to be evaluated by using the same values of accessed parameters under different scenarios as will be demonstrated in Chapter 5. One significant physiological finding has been discovered from the multiple numerical optimization processes and from analyzing a PK profile simulated based on one PK study with fraction excreted to urine data. It was that the renal clearance of the intact cisplatin is only or mostly processed by the passive process, glomerular filtration. This could be due to either an only presence of the glomerular filtration or a situation where all the renal clearances occur but the tubular reabsorption drastically hinders the action of the tubular secretion.

Chapter 5 Model evaluation

5.1 Introduction

Since the main objective of this thesis is to construct a reliable PBPK model that closely represents the real kinetics in agreement with existing observed pharmacokinetics (PK) data of cisplatin for rats and as well as for humans, the validity of the developed model needs to be evaluated by means of validating the simulated values of parameters under diverse settings. This will be discussed in this chapter. The evaluation of the model reliability in this thesis will therefore follow steps of assessing the predictive model operation on cisplatin PK on various rats and humans. Owing to the mechanistic nature of the PBPK model, the extrapolation can be performed by merely modifying the anatomy and physiology of an organism while keeping the physicochemical properties of the drug constant. The only challenge in the extrapolation process is to find the absorption, distribution, metabolism, and excretion (ADME) details that may differ among the species. As an example, the ratio of Kbind1 to Kmet in humans could be different from what has been found in the rat model because humans may have different contents of available albumin or peptides such as glutathione (GSH) in plasma as compared with rats. This is to be investigated during the process of assessing the validity of the PBPK model for humans. The approach taken here is to assume that humans have the same ADME details as rats, generate the PK simulations accordingly, and analyze the predictive utility by comparing the simulated results with observed human PK data. Thus, the same values of the parameters obtained from the rat model are to be applied to the human model in order to preserve the same ADME details prior to analyzing the human PK profiles. The model evaluation will be completed by reviewing predicted values of PK parameters that are specific to one simulation of a PK study, such as total plasma clearance, maximum concentration, and half-life.

5.2 Method

5.2.1 PK Data Acquisition

Nine different PK profiles from two different cisplatin PK study groups have been chosen for evaluation of the rat model [48], [49]. All nine PK profiles contain only cisplatin pharmacokinetics (PK). Therefore, they are more suitable to be used in the model evaluation process because cisplatin PK is the actual resultant or reciprocal element of other cisplatin PK influences such as mobile metabolite PK or fraction unbound, and the detailed PK information for optimizing the parameters is not required at this stage. Four different PK profiles from three different cisplatin PK study groups have been chosen for extrapolating the rat model to human model and evaluating the outcome [16], [18], [50]. The molar mass conversion made for the concentration of species in the plasma during the model development process has also been performed in the model evaluation.

5.2.2 Basic Building Block Setting

Compounds: Cisplatin and Mobile Metabolites

The same virtual compounds, cisplatin and mobile metabolites that have been created during the model development process are used in the model evaluation for both rats and humans. In other words, the same physicochemical properties of cisplatin and mobile metabolites and their ADME settings are adopted for both rats and humans for the purpose of evaluating the developed PBPK model.

Individuals: Rats with Different Weights and Humans with Various Variables

As before, the virtual rats were separately created according to the anatomical data of rats presented in different studies. Weight is the only variable among virtual rats. For the human model, virtual humans were also separately created but with more variables such as ethnicity, gender, age, weight, and height. The mean values of these variables have been used. The metabolic expressions of both rats and humans have been set to link to the three clearances (Kbind1, Kbind2, and Kmet) of cisplatin.

Formulations and Administration Protocols

The same formulation type, 'dissolved' was used for the administration of a dissolved cisplatin solution. As for the administration protocols, different doses and administration types were separately assigned according to the protocols that the pharmacokinetics (PK) studies used. They are all administered with cisplatin as a single dosing interval. The administration protocols for rats and humans that have been used to evaluate the model are shown in Tables 6 and 7.

Table 6: Administration protocols for rats used by cisplatin PK groups

	Administration type	Infusion time (hr) (if applicable)	Dose (mg/kg)
Fukushima et al. [48]	Intravenous (IV) bolus	N/A	7.5
Fukushima et al. [48]	Intravenous (IV) infusion	2	1
Fukushima et al. [48]	Intravenous (IV) infusion	2	2.5
Fukushima et al. [48]	Intravenous (IV) infusion	2	5
Fukushima et al. [48]	Intravenous (IV) infusion	2	7.5
Nagai and Ogata [49]	Intravenous (IV) bolus	N/A	1
Nagai and Ogata [49]	Intravenous (IV) bolus	N/A	5
Nagai and Ogata [49]	Intravenous (IV) infusion	2	5
Nagai and Ogata [49]	Intravenous (IV) infusion	3	5

Table 7: Administration protocols for humans used by cisplatin PK groups

	Administration type	Infusion time (hr) (if applicable)	Dose (mg/m^2)
Verschraagen et al. [16]	Intravenous (IV) infusion	1	75
Andersson et al. [50]	Intravenous (IV) infusion	1	100
Nagai et al. [18]	Intravenous (IV) infusion	2	80
Nagai et al. [18]	Intravenous (IV) infusion	4	80

It is noted that another administration type, the intravenous (IV) infusion that is often used for cancer treatment in the clinic, is introduced in the model evaluation process. Previously in the model development process, the PBPK model has been constructed based on the PK profiles with intraperitoneal (IP) bolus and intravenous (IV) bolus types of administration. Therefore, in the following sections, the model's predictive operations on different types of administration will also be evaluated.

5.3 Result

The simulated values of parameters that have been determined from the model development process are to be validated by conducting several visual predictive checks. As addressed before, the PK profiles reproducing the observed PK data will be simulated by applying the same optimized values of the parameters into both the rat and human models. According to the assumptions made on cisplatin metabolism as described in Chapter 3, the parameters define the absorption, distribution, metabolism, and excretion (ADME) details of cisplatin in an organism. Therefore, validating the optimized values of the parameters is an essential step in cisplatin PBPK modeling and furthermore it may help revealing any unclear mechanism of cisplatin ADME.

5.3.1 Visual Predictive Check with Observed PK Data of Rats

In this section, the last set of optimized values in Figure 7 is applied to the specified rat models describing the nine different PK profiles in order to check the predictive performance in a consistent manner while validating the optimized values of the parameters.
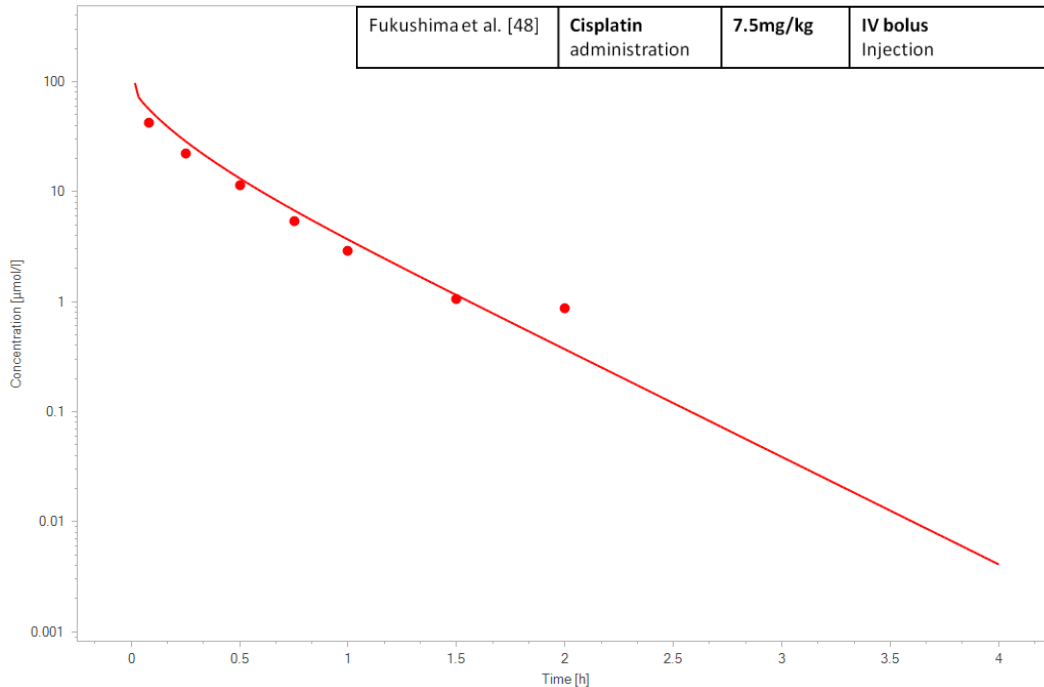
Figure 14: Simulation reproducing experimental PK study by Fukushima et al. [48] showing PK simulation of intact cisplatin (solid line in red); solid dots represent experimentally observed values (generated by Open Systems Pharmacology (2019) platform [9])

Figure 14 illustrates PK simulation of intact cisplatin reproducing the observed PK data by Fukushima et al. [48]. There is an excellent agreement between the simulation and the observed PK data except that the simulation has a slightly higher concentration of cisplatin in the beginning. It should be noted that although the concentration was last observed at 2 hour by Fukushima et al. [48], the end time of the simulation was set to be 4 hour to have the same time scale as other PK simulations adopted in the evaluation of the rat models. The discrepancies in cisplatin concentrations predicted from 2 hours can be considered as insignificantly small, given that the concentration axis is shown with a logarithmic scale as for all other simulations in this thesis.
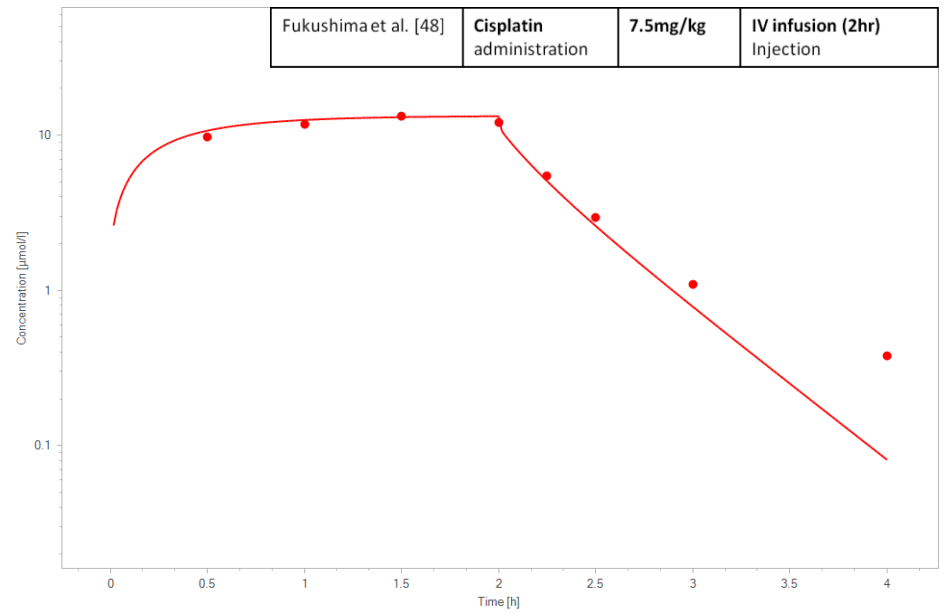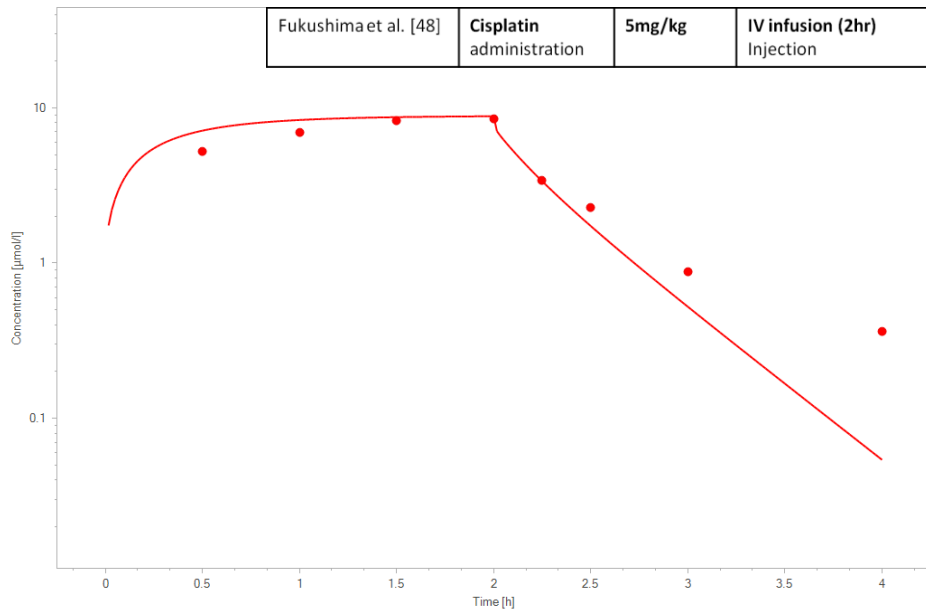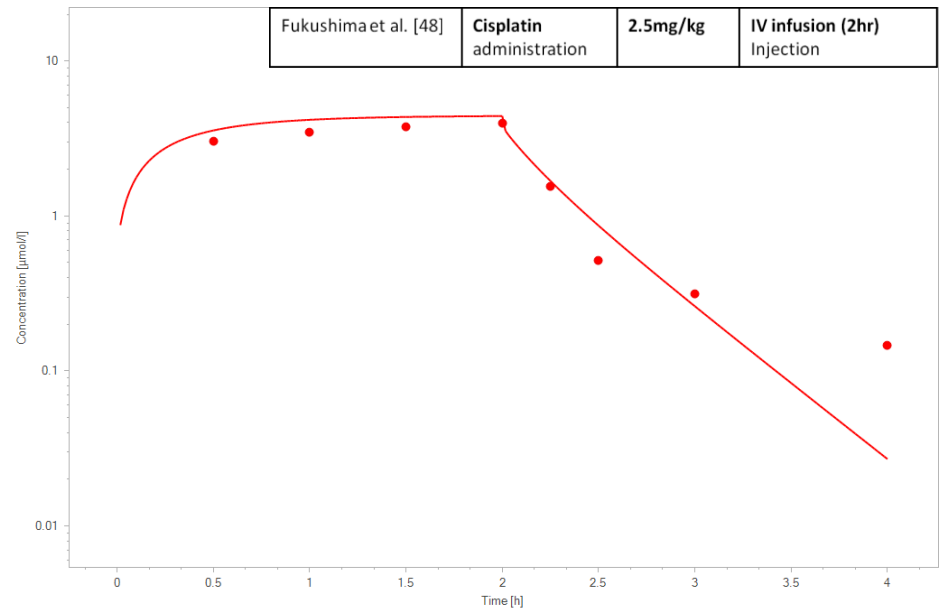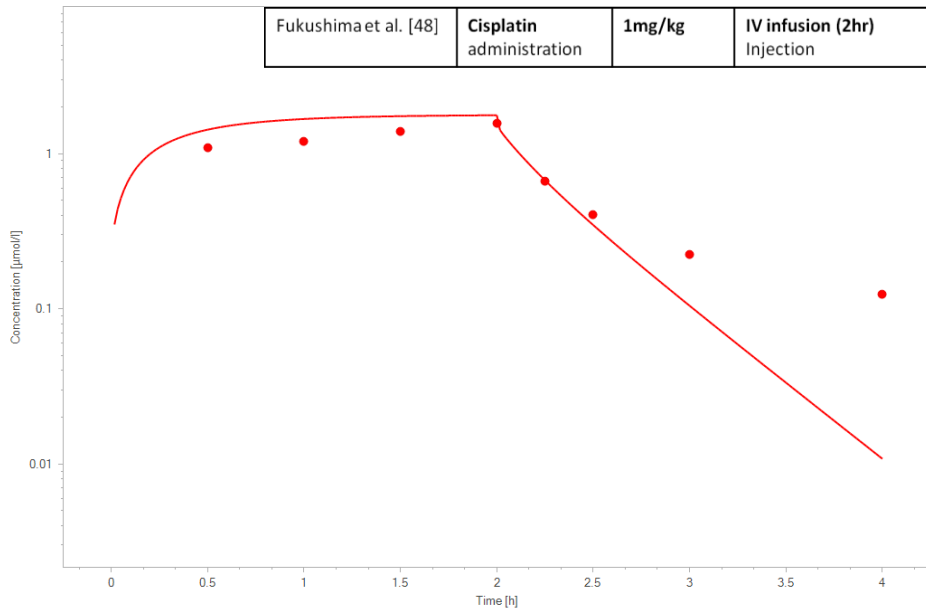
Figure 15: Simulations reproducing experimental PK study by Fukushima et al. [48] showing PK simulations of intact cisplatin (solid line in red) with intravenous (IV) infusion administrations with different doses; solid dots represent experimentally observed values (generated by Open Systems Pharmacology (2019) platform [9])

Four PK profiles of cisplatin pharmacokinetics (PK) with the intravenous (IV) infusion administration have been reproduced from the PK observations by Fukushima et al. [48]. The only administration protocol variance among them is the administered dose. Therefore, the consistency of the model's PK predictions versus different doses can easily be assessed. Following the administration protocols, the infusion times in the simulations are set to be 2 hours and as expected, the highest cisplatin concentrations have been found to be at 2 hours, in agreement with the observed data. As in the case with bolus administration from the same group shown in Figure 14, the initial concentrations have been simulated to be slightly higher until they reach the highest concentrations at 2 hours. However, it can apparently be seen that at a higher administered cisplatin dose, a better agreement between the simulation and observed data is found. Additionally, by observing higher cisplatin concentrations simulated for higher administered doses and vice versa, with excellent agreements between the four simulations and the four observed PK data, it can be found that the PBPK model maintains the consistency of the PK predictions independent of administered doses, as expected from Equation 2.

Another PK study group, Nagai and Ogata [49] conducted a similar experiment where they observed cisplatin PK with administrations of IV bolus and IV infusion but with different infusion times rather than the administered dose. The next visual predictive checks of the PBPK model are shown in Figure 16.
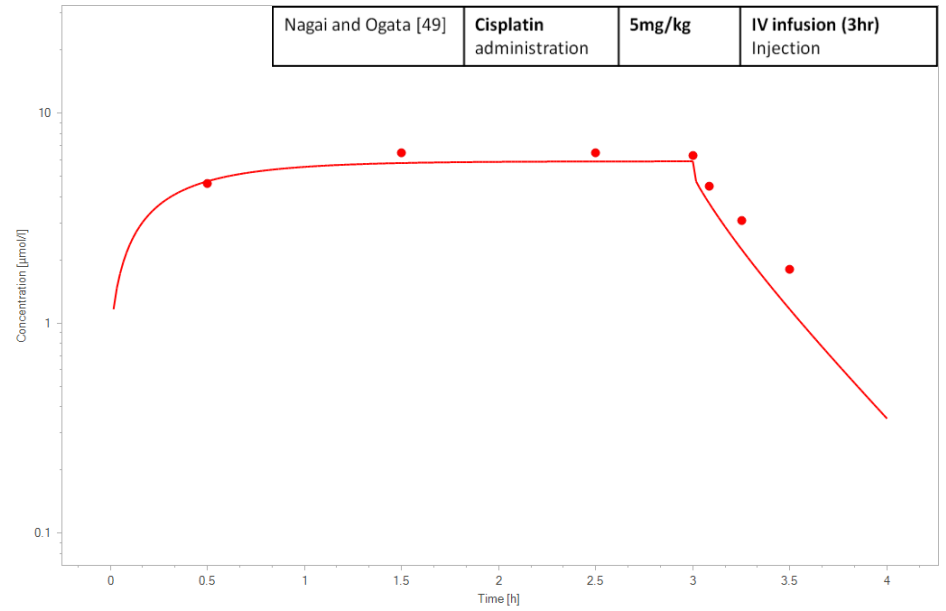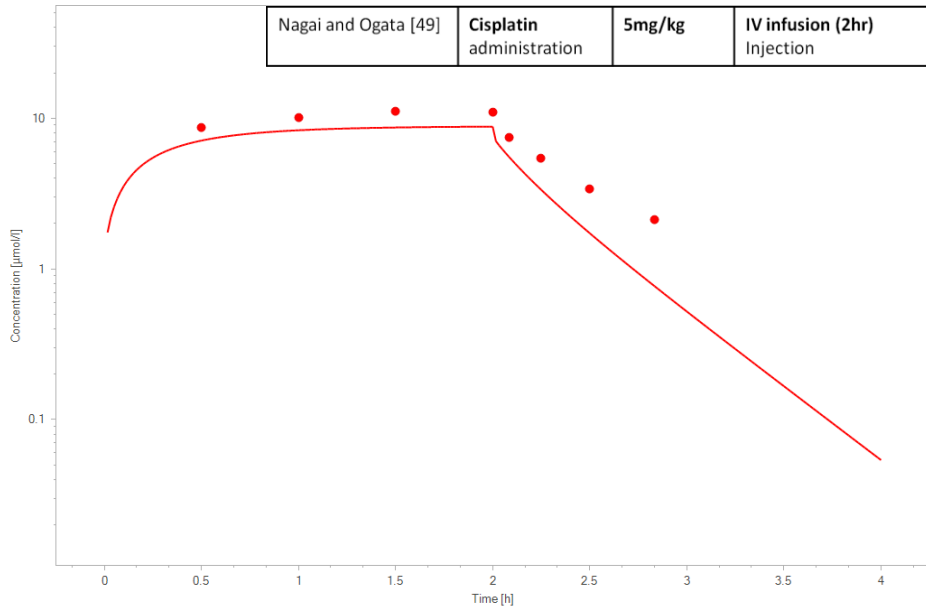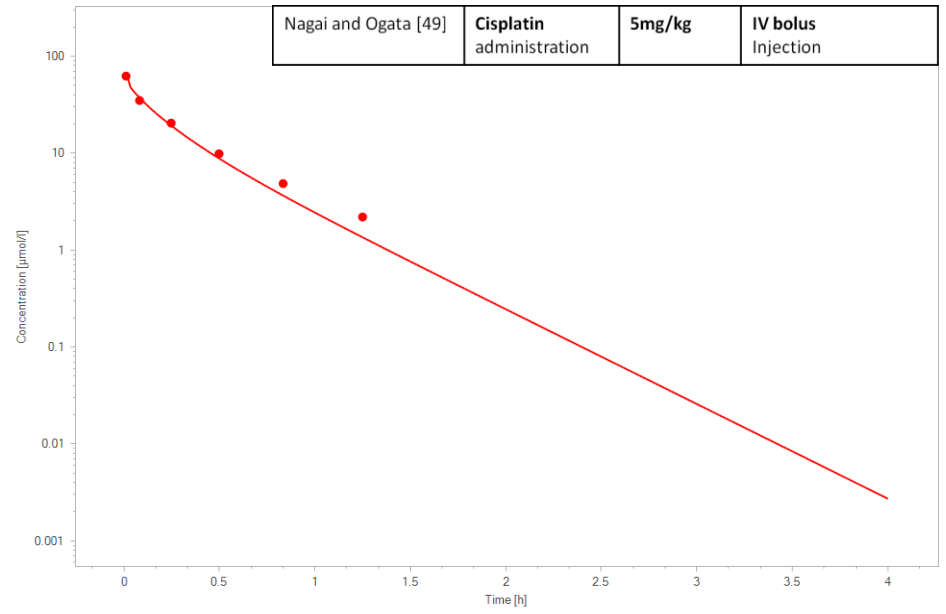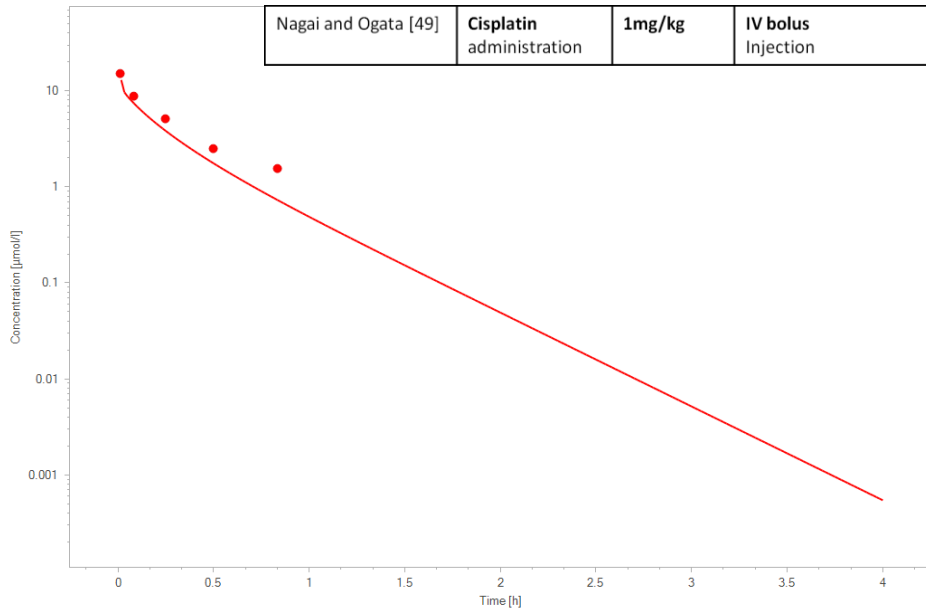
Figure 16: Simulations reproducing experimental PK study by Nagai and Ogata [49] showing PK simulations of intact cisplatin (solid line in red) with administrations of intravenous (IV) bolus and intravenous (IV) infusion with different infusion times; solid dots represent experimentally observed values (generated by Open Systems Pharmacology (2019) platform [9])

The two simulations with the intravenous (IV) bolus administrations gave almost exactly the same starting concentration data points as those observed by Nagai and Ogata [49]. Among all the observed PK data that have been used in this thesis, these two datasets with the IV bolus administration provided the earliest observed time (45 seconds) which made it possible to evaluate the PBPK model's predictive performance even at the very starting time of the injection. Based on the results as shown, it can be concluded that the model is very accurate at the outset of the injection as it is supposed to be, given that the exact administration protocol is followed. As it was found from the visual predictive check with the PK data with the IV infusion administration observed by Fukushima et al. [48], the simulation here with the IV bolus administrations with higher administered dose also align better with the observed data. Therefore, it can be deduced that with administration of higher cisplatin doses, better agreements between the simulation and observed PK data can be achieved for administrations of both IV bolus and IV infusion and possibly for other administration methods as well.

Comparing the two simulations with IV infusion administrations generated based on the observed PK data by Nagai and Ogata [49], it can be found that the infusion time may also be a factor that affects the extent of the model agreement with the observed data. The simulation with infusion time of 3 hours as compared with the simulation with infusion time of 2 hours aligns better with the corresponding observed data.

5.3.2 Validity of the PBPK Model for Humans

As previously mentioned, the human model can be easily constructed based on the constructed rat model by only modifying the anatomy and physiology. Therefore the virtual rat is replaced with a virtual human and the physicochemical properties of cisplatin and mobile metabolite remain the same in the human model. Moreover, for the purpose of assessing the validity of the model's predictive utility for extrapolation from rats to humans, it was assumed that humans have the same absorption, distribution, metabolism, and excretion (ADME) details of cisplatin that were found in rats. So the same optimized values of the parameters are applied to the human model to preserve the ADME details.

The human model evaluation process is conducted based on four observed human PK profiles of which some present more detailed PK information other than intact cisplatin pharmacokinetics (PK) data. Due to the difficulty, unnecessity, or inefficiency of using sophisticated techniques to collect PK of species other than intact cisplatin (e.g mobile metabolite or fixed metabolite) on humans, the relevant human PK data are very limited. One found PK data adopted in this thesis required several calculations for more PK details.
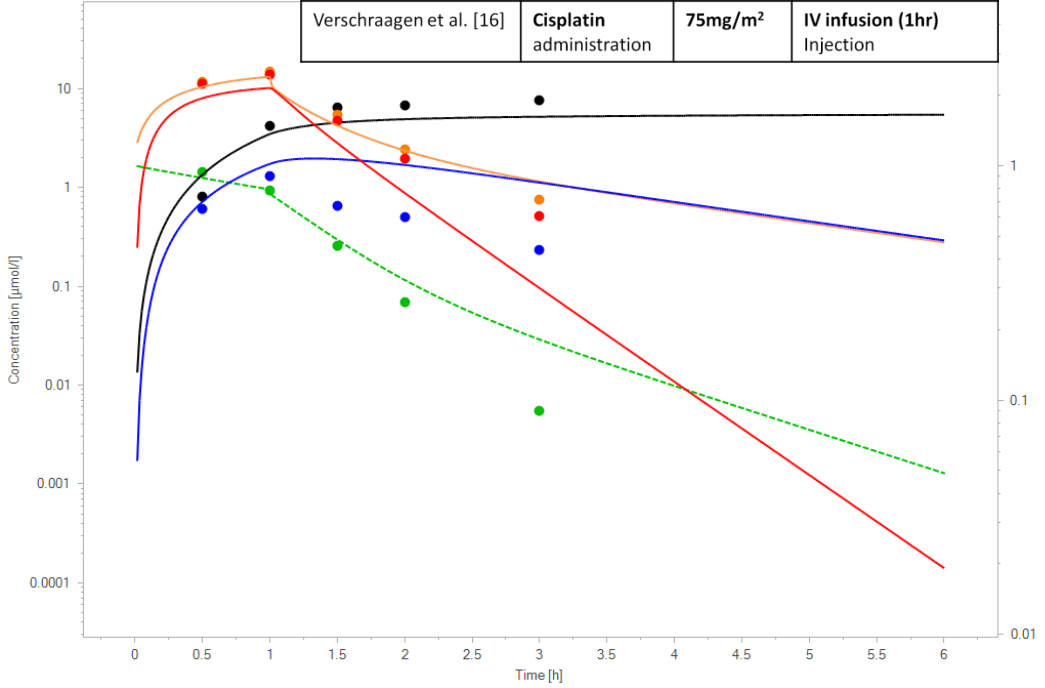
Figure 17: Simulation reproducing experimental PK study by Verschraagen et al. [16] showing PK simulations of intact cisplatin (solid line in red), ultrafilterable platinum (solid line in orange), mobile metabolite (solid line in blue), fixed metabolite (solid line in black), and fraction unbound (dotted line in green); solid dots represent experimentally observed values (generated by Open Systems Pharmacology (2019) platform [9])

It should be noted that Verschraagen et al. [16] only presented pharmacokinetics (PK) of intact cisplatin, ultrafilterable platinum, and total platinum. The total platinum is a sum of all unbound and bound species containing the platinum. Thus, following the definitions described in section 3.3.2, it is a sum of ultrafilterable platinum and fixed metabolite. Therefore, the fixed metabolite data could be estimated as:

$$\text{Fixed metabolite} \quad = \quad \text{Total platinum} \quad - \quad \text{Ultrafilterable platinum} \qquad (12)$$

Based on Equation 11, the fraction unbound data could also be estimated as:

$$\text{Fraction unbound} \quad = \quad \frac{[\text{Ultrafilterable platinum}]}{[\text{Total platinum}]} \qquad (13)$$

Lastly, the mobile metabolite data could be estimated as:

$$\text{Mobile metabolite} \quad = \quad \text{Ultrafilterable platinum} \quad - \quad \text{Intact cisplatin} \quad (14)$$

Therefore, it should be emphasized that the three sets of the PK data points for fixed metabolite, fraction unbound and mobile metabolite are only estimated using Equations 12, 13, and 14 respectively and they are not actual observed data.

54

The comparisons of the two simulations with observed PK data granting more reliable assessments are firstly made. It appears that the ultrafilterable platinum pharmacokinetics (PK) has been extrapolated quite accurately while cisplatin PK has been simulated to have slightly lower concentrations than the observed values. Observing the small differences between the observed data points of the ultrafilterable platinum and those of the intact cisplatin, it can be suspected that the intact cisplatin is not readily metabolized in humans. This observation is very different from what was observed by Yates and McBrien [15] for cisplatin PK study with rats where it showed high metabolizing activity with intact cisplatin at the start of administration as shown in Figure 10.

Given that mobile metabolite concentration is the difference between the ultrafilterable platinum concentration and the intact cisplatin concentration, the mobile metabolite PK has been simulated to have higher concentrations than the observed values of the mobile metabolite as expected. In other words, the wider gap between the two PK simulations of ultrafilterable platinum and intact cisplatin results the higher mobile metabolite concentration while the narrower gap between the two data points results the smaller mobile metabolite concentration.

The fixed metabolite is a product of albumin / intracellular protein / DNA binding from both intact cisplatin and mobile metabolite handled by Kbind1 and Kbind2 respectively. During the PBPK model development process, Kbind1 (0.00284 l/h) was optimized to be about 3 times higher than Kbind2 (0.000974 l/h) implying that the fixed metabolite is accumulated 3 times more from the intact cisplatin binding, or the fixed metabolite accumulation in the simulation is more contributed from the intact cisplatin PK simulation. Therefore, the fixed metabolite PK has been simulated to have lower concentrations than the concentrations from the data.

An excellent agreement is found between simulated fraction unbound and the estimated data of the fraction unbound. The exact match at 1 hour (fraction unbound of 0.78) is very surprising and the extrapolating trends thereafter are also very similar. This excellent result could be expected from the observations of the alignments between simulations of both ultrafilterable platinum PK and fixed metabolite PK and the corresponding data since the fraction unbound is defined to be composed of only the two PK concentrations as shown in Equation 11 or 13.
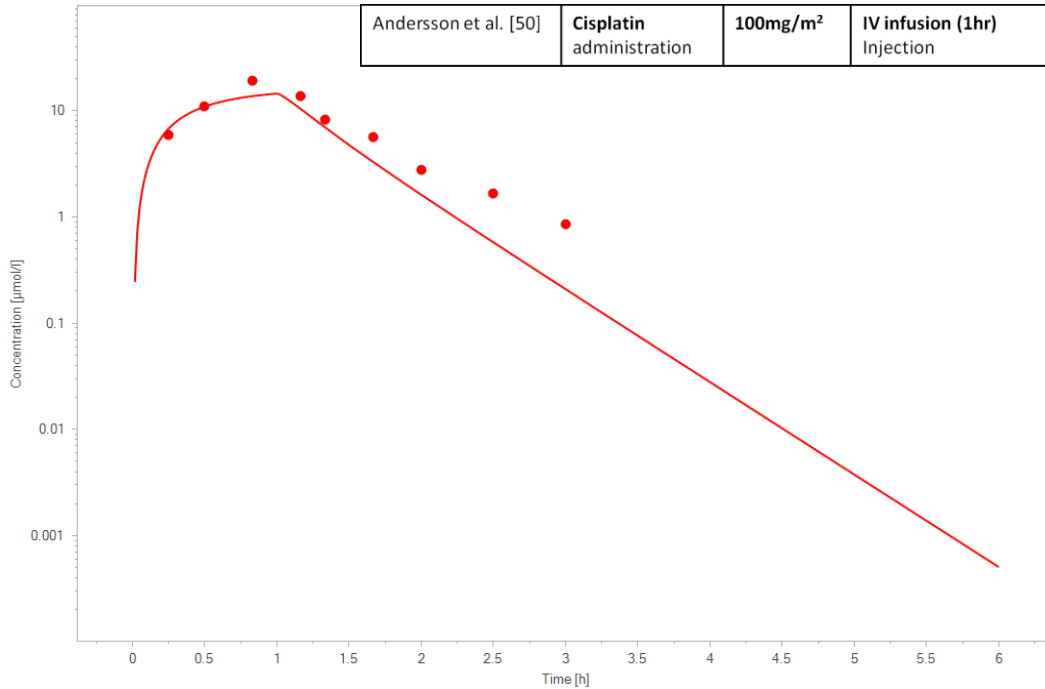
Figure 18: Simulation reproducing experimental PK study by Andersson et al. [50] showing PK simulation of intact cisplatin (solid line in red); solid dots represent experimentally observed values (generated by Open Systems Pharmacology (2019) platform [9])

Figure 18 illustrates PK simulation of intact cisplatin reproducing the observed PK data by Andersson et al. [48]. The intact cisplatin PK is accurately reproduced, particularly in the beginning of the simulation. However, the maximum cisplatin concentration was not observed at 1 hour as it is expected for the 1 hour infusion time-administration protocol, and accordingly a discrepancy occurred with the simulation at that point. Cisplatin elimination trend is well predicted noting the logarithmic scale concentration axis. For instance, at 3 hours, the largest gap between the observed data point and the simulation is observed, but the concentration difference is only 0.64 μmol/l (Data point: 0.85 μmol/l, simulation: 0.21 μmol/l).
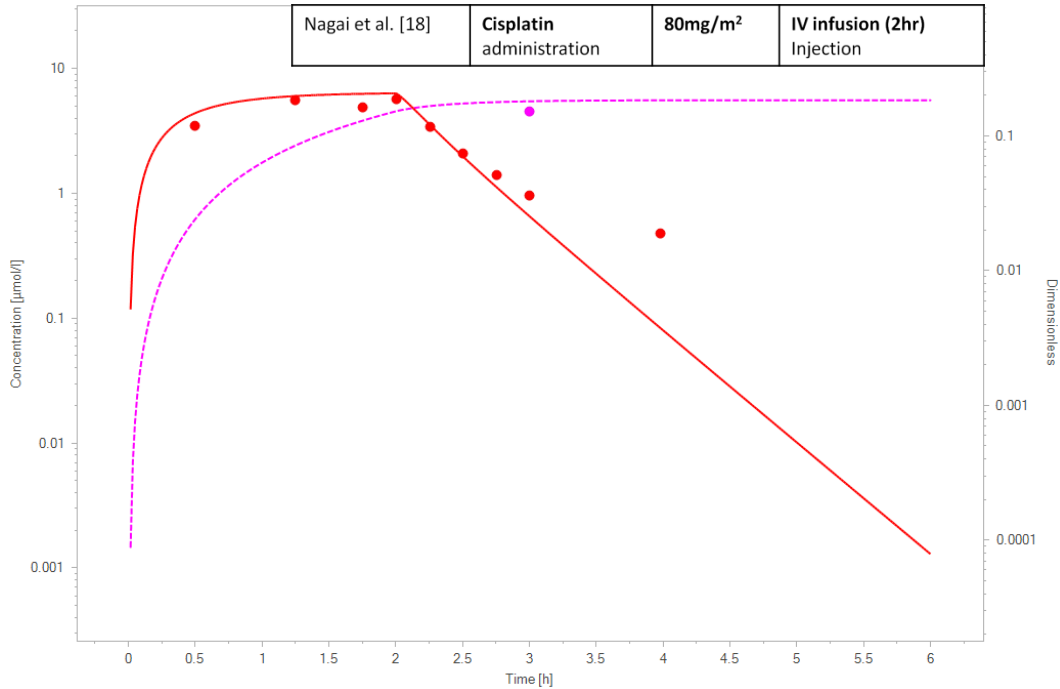
Figure 19: Simulation reproducing experimental PK study by Nagai et al. [18] showing PK simulations of intact cisplatin (solid line in red), and fraction excreted to urine (dotted line in pink); solid dots represent experimentally observed values (generated by Open Systems Pharmacology (2019) platform [9])

Figure 19 illustrates PK simulation of intact cisplatin and fraction excreted to urine, reproducing the observed PK data by Nagai et al. [18]. Based on the comparison between cisplatin pharmacokinetics (PK) simulation and the observed data in the figure, it must be stated that the PBPK model constructed based on the rat PK data has been successfully extrapolated to fit the data for humans. The fraction excreted to urine has also been reproduced very precisely. At 3 hours, the fraction excreted to urine was observed to be 0.15 whereas the simulation produces 0.18.
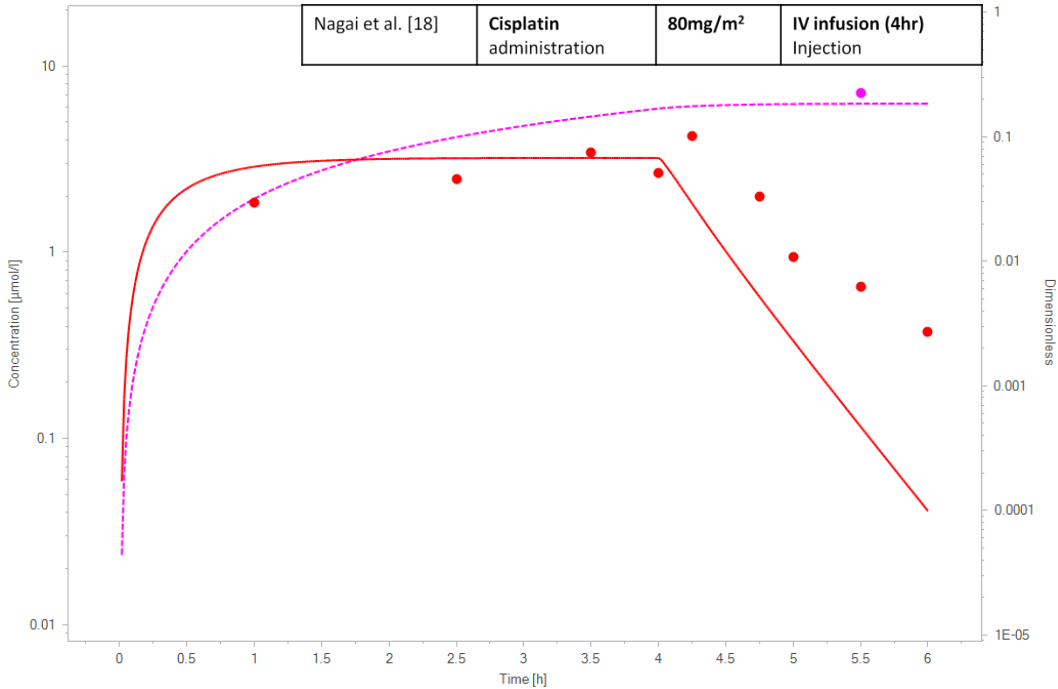
**Figure 20: Simulation reproducing experimental PK study by Nagai et al. [18] showing PK simulations of intact cisplatin (solid line in red), and fraction excreted to urine (dotted line in pink); solid dots represent experimentally observed values (generated by Open Systems Pharmacology (2019) platform [9])**

Figure 20 illustrates PK simulations of intact cisplatin and fraction excreted to urine reproducing the observed PK data by Nagai et al. [18]. The same administration protocol was followed by the group except for the infusion time when compared to the PK study shown in Figure 19. The maximum cisplatin concentration was not observed at 4 hours for the 4 hour infusion time-administration protocol and rather it appears as if cisplatin pharmacokinetics (PK) data was recorded about 30 minutes later than actually observed. It is noted that cisplatin concentration discrepancies found here do not agree with the finding from section 5.3.1 that cisplatin PK may be more accurately simulated for the administration protocol with longer infusion time. The fraction excreted to urine, however, has been reproduced in agreement with the observed data.

5.3.3 Prediction of Fraction Unbound, Responsible for Therapeutic Effect

As addressed in Chapter 4, an 'actual' fraction unbound for cisplatin which is responsible for therapeutic effect in the anticancer treatment is investigated in this section. After an administration of cisplatin, the fraction unbound for cisplatin measures the fraction of unbound cisplatin over all unbound and bound cisplatin in plasma over the time course of PK analysis, as defined in Equation 10. Since the two experimental PK studies of cisplatin by Fukushima et al. [48] and by Nagai et al. [18] have been reproduced the most closely by the PBPK model as shown during the model evaluation processes for rats and humans respectively (Figures 14, 15, and 19), they have been chosen to investigate the fraction unbound for cisplatin by simulating the predicted values.

Figures 21 and 22 show simulations reproducing cisplatin PK study on rats by Fukushima et al. [48] and simulation of the predicted fraction unbound for cisplatin. The fraction unbound for cisplatin is represented by dotted line in purple and the fraction unbound for platinum species which has been used for the purpose of accessing parameters is also shown for comparison.
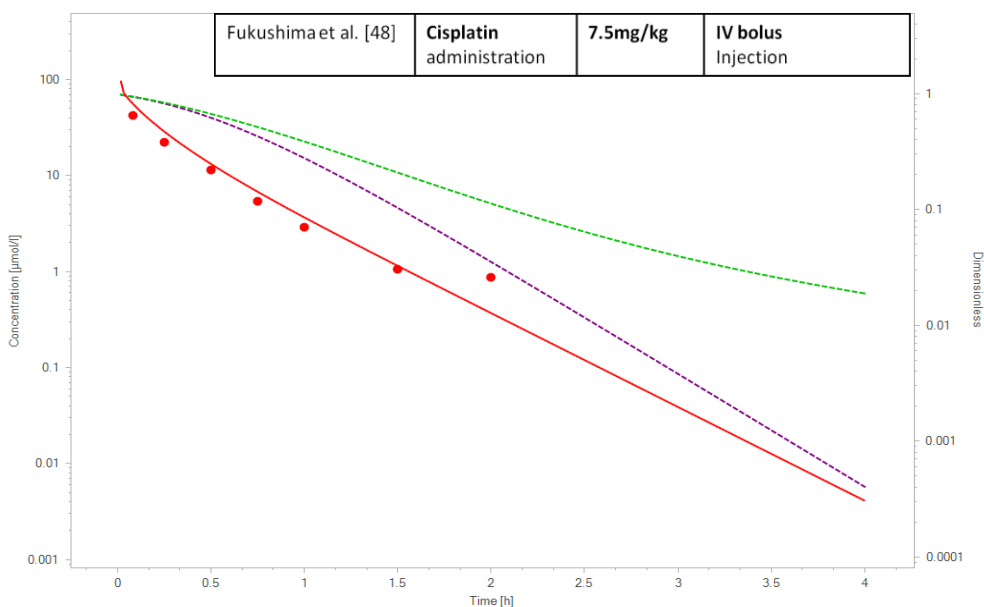

Figure 21: Simulation reproducing experimental PK study by Fukushima et al. [48] showing PK simulations of intact cisplatin (solid line in red), fraction unbound for platinum species (dotted line in green), and fraction unbound for cisplatin (dotted line in purple); solid dots represent experimentally observed values (generated by Open Systems Pharmacology (2019) platform [9])
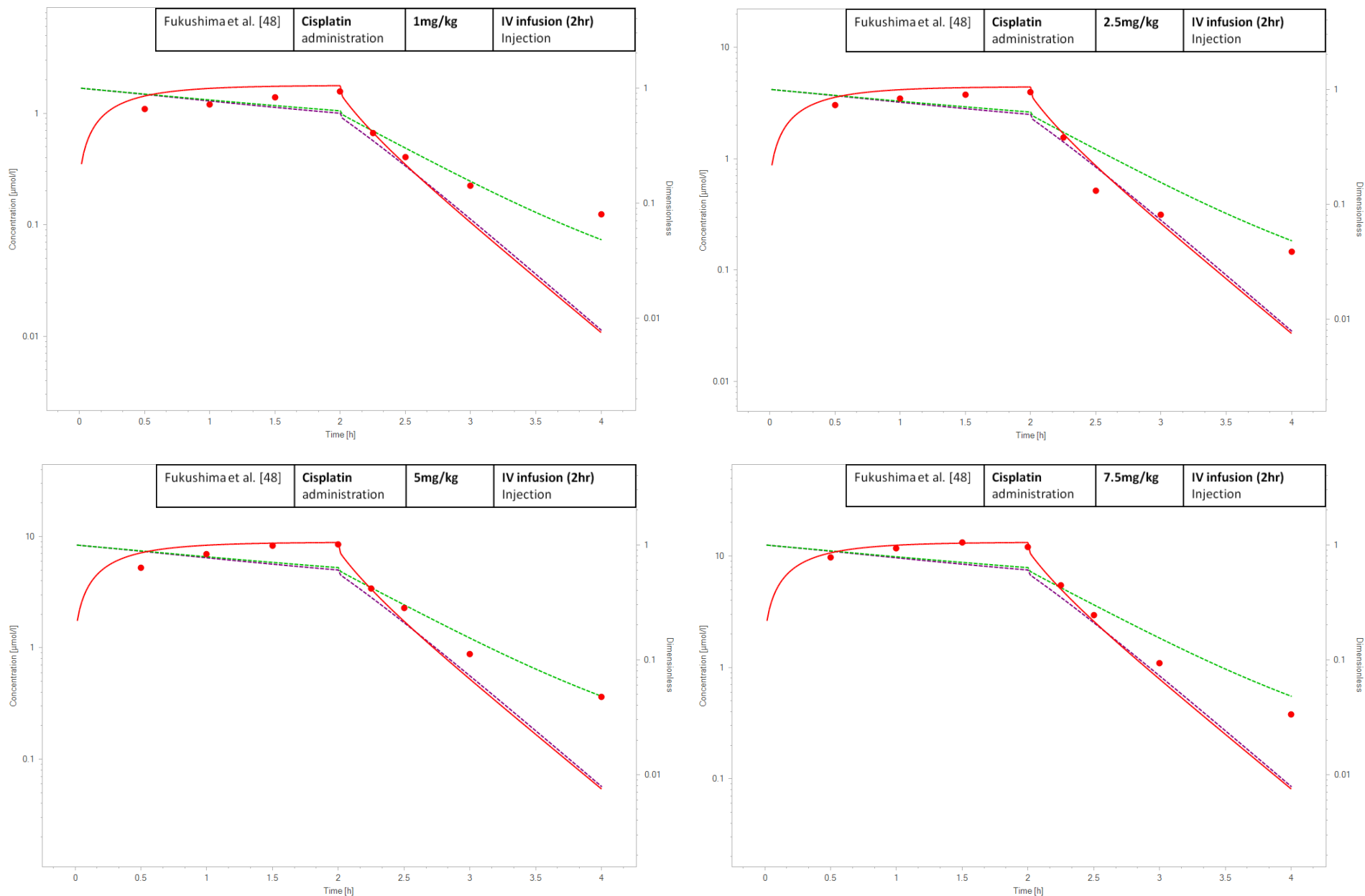
Figure 22: Simulations reproducing experimental PK study by Fukushima et al. [48] showing PK simulations of intact cisplatin (solid line in red), fraction unbound for platinum species (dotted line in green), and fraction unbound for cisplatin (dotted line in purple) with intravenous (IV) infusion administrations with different doses; solid dots represent experimentally observed values (generated by Open Systems Pharmacology (2019) platform [9])

Notably, an 'actual' fraction unbound for cisplatin decreases faster as it accounts for the concentration of unbound cisplatin only while the fraction unbound for platinum species (or ultrafilterable platinum) accounts for both unbound cisplatin and unbound mobile metabolite. All simulations in Figure 22 show that the two fraction unbound simulations almost align with each other until the end of infusion time then split from that point implying that significant cisplatin metabolic process is occurring. It should be noted that while cisplatin is administered, the fraction unbound for platinum species is only slightly higher because it accounts not only unbound mobile metabolite but also bound mobile metabolite which results greater amount of accumulated fixed metabolites as compared with that in the case of measuring the fraction unbound of cisplatin.
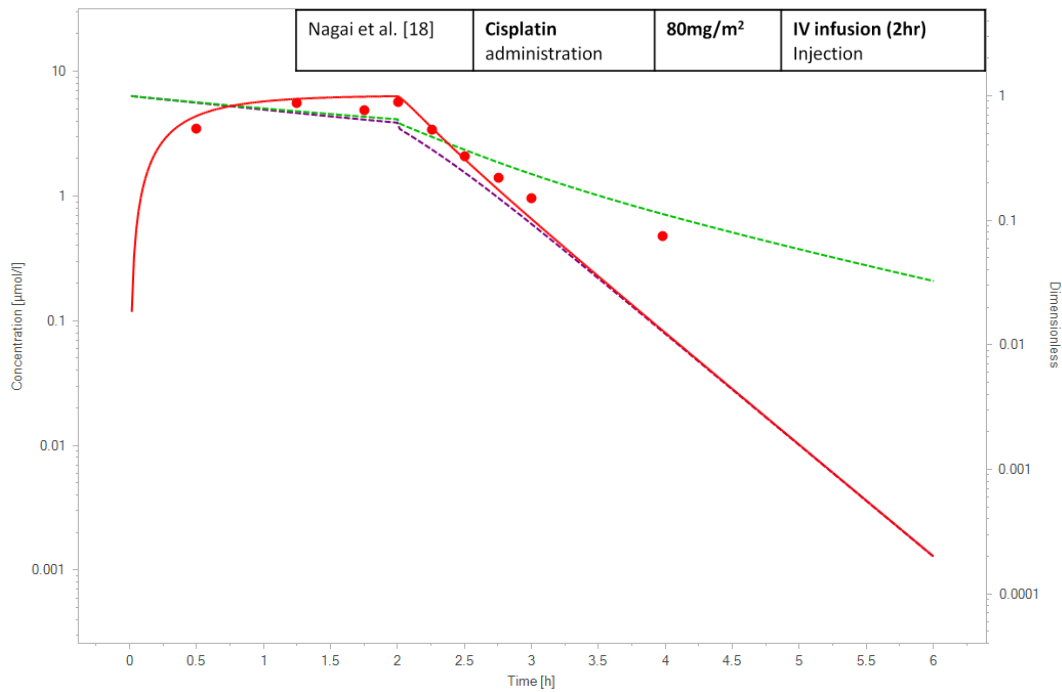

Figure 23: Simulation reproducing experimental PK study by Nagai et al. [18] showing PK simulations of intact cisplatin (solid line in red), fraction unbound for platinum species (dotted line in green), and fraction unbound for cisplatin (dotted line in purple); solid dots represent experimentally observed values (generated by Open Systems Pharmacology (2019) platform [9])

Figure 23 shows a simulation reproducing cisplatin PK study on humans by Nagai et al. [18] and simulation of the predicted fraction unbound for cisplatin. The same aspect of the two fraction unbound simulations observed around the end of infusion time indicates that cisplatin metabolism of humans may be very comparable to that of rats.

5.3.4 PK Analysis by Comparing PK Parameters

As a last step in the model evaluation, predicted values of PK parameters are assessed by comparing with observed data. The PK parameters such as total plasma clearance, and half-life are PK study specific and are not intrinsic to a particular drug or organism. It should be noted that not all experimental PK studies with cisplatin adopted in this thesis provided a set of PK parameters, and therefore the comparisons were made only with those that are available.

Table 8 and 9 show the PK parameter comparisons conducted for the purpose of evaluating the PBPK model and the PK parameters are defined as:

- CL_{tot} (ml/min/kg) :   Total plasma clearance
- $V_{d,ss}$ (ml/kg) :   Aparent volume of distribution at steady-state
- AUC (μmol*min/l) :   Area under the curve from the start to specified time
- C_{max} (μmol/l) :   Maximum drug concentration in plasma
- t_{max} (h) :   Time at which C_{max} occurs
- $t_{1/2}$ (h) :   Half-life
- MRT (h) :   Mean residence time

Table 8: PK parameter comparison on rats

Rat	Nagai et al [12] (Bolus 5mg/kg)		Fukushima et al [37] (Bolus 5mg/kg)		Okada et al [38] (Bolus (5mg/kg)		Nagai and Ogata [42] (Bolus 5mg/kg)		Nagai and Ogata [42] (2h-infusion 5mg/kg)		Nagai and Ogata [42] (3h-infusion 5mg/kg)	
	Simulation	Observed data	Simulation	Observed data	Simulation	Observed data	Simulation	Observed data	Simulation	Observed data	Simulation	Observed data
CL_tot (ml/min/kg)	18.81	17.55	18.72	24	18.69	28.28	18.74	15.8	15.67	13.3	15.67	14.6
V_d,ss (ml/kg) (Obtained from phys-chem parameters)	399.25, 751.68		397.86, 751.68		397.21, 751.68	784	398.06, 751.68		279.47, 751.68		279.08, 751.68	
AUC (umol*min/l) (Mobile metabolite)	886.15 (inf) 245.99 (inf)	999.57 (inf) 254.25 (inf)	883.44 (2h)	719.89 (2h)	885.23 (2h)	606.57 (2h)	853.74 (1.25 h)	1079.02 (1.25h)	1043.22 (2.83h)	1255.87 (2.83h)	1034.27 (3.5h)	1149.25 (3.5h)
C_max (umol/l)	64.95	57.89 IV Bolus	65	30.76 IV Bolus	65.03	24.13 IV Bolus	64.99	62.33 IV Bolus	8.81	11.69	5.91	6.92
t_max (h)	0.02	0.02 IV Bolus	0.02	0.08 IV Bolus	0.02	0.08 IV Bolus	0.02	0.01 IV Bolus	2	2	3	3
t_1/2 (h)	0.31		0.31		0.31	0.715	0.31		0.31		0.3	
MRT (h)	0.35		0.35		0.35		0.35	0.387	0.3	0.41	0.3	0.475

Table 9: PK parameter comparison on humans

Human	Verschraagen et al [11] (1h-infusion 75mg/m2)		Andersson et al [43] (1h-infusion 100mg/m2)		Nagai et al [13] (2h-infusion 80mg/m2)		Nagai et al [13] (4h-infusion 80mg/m2)	
	Simulation	Observed data	Simulation	Observed data	Simulation	Observed data	Simulation	Observed data
CL_tot (ml/min/kg)	9.77	12.32	8.91	7.96	10.07	13.09	10.11	9.69
V_d,ss (ml/kg) (Obtained from phys-chem parameters)	239.41, 653.81	290	249.02, 702.83	281.86	269.03, 725.95		270.05, 726.56	
AUC (umol*min/l) (Mobile metabolite)	667.34 (6h)	930 (6h)	976.97 (3h)	1066.5 (3h)	769.84 (inf)	655.9 (inf)	770.61 (inf)	815.87 (inf)
C_max (umol/l)	10.14	13.7	14.42	14.33	6.33	7.4	3.21	4.63
t_max (h)	1	0.94	1	0.83	2	2	4	4
t_1/2 (h)	0.32	0.47	0.34	0.38	0.34	0.41	0.33	0.59
MRT (h)	0.41	0.67	0.47		0.45	0.78	0.45	1.38

The dark grey shade in the table indicates that the data for the particular PK parameter is not available from the study. The orange shade in the table indicates that the presented value obtained from the PK study with the IV bolus method may not be reliable. The IV bolus always gives the C_max, the maximum drug concentration in plasma at the very starting time of the administration, and it does not necessarily mean that the first data point presented is actually obtained at the starting time of the administration due to a technical difficulty or unnecessity of obtaining the C_max in a PK study.

Unit conversions have been made to follow default units given by the Open Systems Pharmacology platform. Mass units were converted to molar units using the molecular weight of cisplatin mobile metabolite or platinum as demonstrated in Equation 6. For example, AUC (mg*min/L) or C_max (ug/mL) was converted to AUC (μmol*min/l) or C_max (μmol/l). Another conversion method had to be applied to convert the human equivalent dose or body surface area (BSA) dose (ie. mg/m^2) to animal dose (ie mg/kg). FDA guideline recommends the following conversion method [51]:

$$\text{mg/m}^2 = \text{km} * \text{mg/kg} \qquad\qquad (15)$$

$$\text{where km is a body weight (W) specific factor, km} = 9.09 * \text{W}^{0.35}$$

As an example, in cisplatin PK study by Andersson et al. [50], the total plasma clearance was provided as 0.32 L/min/m^2 and the mean body weight of the seven patients was calculated to be 69.86kg. Therefore the unit conversion is made as:

$$\text{km} = 9.09*(69.86)^{0.35} = 40.2 \text{ kg/m}^2 \qquad\qquad (16)$$

$$\text{therefore AUC} = \frac{0.32 \text{L/min/m2}}{40.2 \text{ kg/m2}} * \frac{1000 \text{ mL}}{1\text{L}} = 7.96 \text{ ml/min/kg}$$

Generally, those PK studies that showed excellent agreements between the simulations and observed PK data also provided very similar PK parameter values as expected. Particular examples would be the PK studies shown in the first and last columns in Table 8 (for rats) and the second column in Table 9 (for humans) showing very similar values of CL-tot and AUC.

5.4 Conclusion

The PBPK model that was constructed based on the rat PK data has been evaluated by conducting the predictive check with more rat PK data and also with human PK data after extrapolating to a human model. From the evaluation process with the rat model, it was found that for administrations of both intravenous (IV) bolus and IV infusion, the model showed better predictive performance on cisplatin pharmacokinetics (PK) at a higher administered dose. The model also reasonably shows the consistency of the PK predictions independent of administered doses, as shown in Figures 15 and 16. Overall, the rat PK data have been well reproduced with high precision in cisplatin elimination trend in plasma represented as the slope in the plot. For the PK studies with the IV infusion administration, cisplatin accumulation trend up to the point of infusion end time is also well described in the simulations.

The purpose of evaluating the PBPK model on humans is to validate the model's predictive utility for extrapolation from rats to humans. Therefore, the optimized values of the parameters that had already been evaluated from the rat model needed to be re-evaluated by applying them into a human model and assessing cisplatin PK reproducibility on humans. The same predictive check procedure was followed and the level of reproducibility of cisplatin PK on humans appeared to be comparable with that on rats. There was one disagreement found between a simulation and the PK observed data but the data did not seem to agree with general PK observation that the maximum drug concentration is found at the end of the infusion time. However, other PK profiles including fraction unbound and fraction excreted to urine have been reproduced precisely. The results could be verified by comparing the PK parameters predicted from the simulations and those from the observed PK data. Therefore, the conclusions would be that the PBPK model has been validated for its predictive performance on cisplatin PK on humans and the absorption, distribution, metabolism, and excretion (ADME) of cisplatin that are defined by the parameters may be similar in both species, rats and humans.

Chapter 6 Conclusions

6.1 Summary

A physiologically based pharmacokinetic (PBPK) model of cisplatin has been constructed, and evaluated according to a proposed PBPK modelling framework. The validity of predictive utility for extrapolating from a rat model to a human model has also been assessed. The model could adequately characterize and reproduce the pharmacokinetics (PK) of cisplatin in plasma for both rats and humans based on observed PK data. This confirmed that the assumptions made on absorption, distribution, metabolism, and excretion (ADME) details of cisplatin prior to constructing the model are reliable upon the successful validation of the parameters from the model evaluation processes.

6.1.1 Reproducibility of Cisplatin PK by PBPK model

The constructed PBPK model has been evaluated for its predictive performance on rats and humans by assessing the reproducibility of cisplatin PK based on observed data. It must be emphasized that reproducibility of other species PK or fraction data can also be observed simultaneously given that the PBPK model is mechanistically structured to describe the kinetics of cisplatin-metabolized products that are pharmacologically related. For example, ultrafilterable platinum PK is formulated to be simulated as a sum of concentrations of intact cisplatin and mobile metabolite over the course of the PK analysis.

Repeatability is assessed from multiple measurements of the same methods by the same observers so any variability should come from a possible measurement error. Reproducibility is assessed from multiple measurements of the same methods but by different observers so there may exist systemic bias between observers. The physiologically based pharmacokinetic (PBPK) model will always generate the same PK simulation following one particular administration protocol. Therefore, it can be useful in comparing and analyzing PK profiles that are observed by different study groups or by the same group at different times but all with the same administration protocol followed. In other words, the PBPK model can also be a great tool to assess repeatability and reproducibility of PK profiles when the experimental data are observed by following the same administration protocol. For example, during the model development process, the reproducibility of cisplatin PK was discussed on the two data separately observed by Fukushima et al. [44] and Okada et al. [45] (Figures 12 and 13) by comparing them to the simulation generated following the same administration used by the two groups.

Reliability on the other hand is assessed from different measurement methods. The PBPK model has been constructed based on rat PK datasets obtained with administrations of Intraperitoneal (IP) bolus and Intravenous (IV) bolus and it has been evaluated based on observed PK datasets which followed different administration protocols such as different cisplatin dose amount and/or IV infusion administration. The model has also been evaluated for its modality of interspecies extrapolation from rat to human model by using human PK datasets. This thesis is essentially about testing the reliability of the PBPK model of cisplatin under various clinical settings with cisplatin.

From the model evaluation process, it was found that the reproducibility of cisplatin PK by the PBPK model is slightly higher for an administration protocol with higher cisplatin dose. This was confirmed from both cases of IV bolus and IV infusion administrations. Given that the PBPK model is constructed to consistently simulate cisplatin PK regardless of dose amount, there could be a measurement error at low dose of cisplatin administrations. More significantly, the better reproducibility of cisplatin PK found at a higher dose shows that the nonlinear kinetics of cisplatin does not exist indeed. If the nonlinear kinetics of cisplatin exists, cisplatin PK would encounter the nonlinearity when higher doses of cisplatin are administered. In other words, at

higher doses of administration, there would be more significant discrepancies found between simulated and observed PK data because the PBPK model is constructed to always follow the linear first order kinetics regardless of the dose, as described in Chapter 4. The better agreement achieved at a higher dose implies that cisplatin PK in fact follows the linear kinetics, validating the first order linearity assumption made in the model.

From evaluating the rat model, it was also found that the reproducibility of cisplatin PK is higher for a longer infusion time so the infusion time may also be another factor for the predictive performance but this finding was disagreed by the human model which did not closely reproduce the human data with the longer infusion time. It was argued that there may have been a measurement error with the observed PK data pointing that the maximum drug concentration was not found at the end of the infusion time. This finding is subject to be investigated with more available human PK data in a future project.

6.1.2 Analysis of the Parameters

During the PBPK model development process, physiological relevance has been identified. One of the parameters, TSmax for cisplatin was pronounced to be not uniquely identifiable from multiple numerical optimization processes and its optimized value was found to be about six orders of magnitude less than the optimized value of TSmax for mobile metabolite implying that the tubular secretion of cisplatin may not be a significant contribution to the urine excretion of intact cisplatin. Conclusion was made that the intact cisplatin is renally cleared by either glomerular filtration (passive process) only or all the renal clearance processes: glomerular filtration, tubular secretion (active process), and tubular reabsorption (active process) but the action of the tubular secretion is drastically hindered by the tubular reabsorption.

Another finding on cisplatin metabolism may be established by comparing the optimized values of the parameters that represent binding and metabolizing rates:

$$Kmet\ (0.01\ l/h) > Kbind1\ (0.00284\ l/h) > Kbind2\ (0.000974\ l/h) \qquad (17)$$

As shown in Equation 17, the intact cisplatin is metabolized at the highest rate compared to the rates of fixed metabolite formations. This explains the slow accumulation of the fixed metabolite relative to the rapid elimination of the intact cisplatin as shown in Figures 8 and 17.

By comparing the optimized values of Kbind1 and Kbind2, it can be found that compared to the mobile metabolite, the intact cisplatin binds with higher affinity to albumin, intracellular protein, or DNA. This was expected as both simulation and observed data of PK profiles presenting pharmacokinetics (PK) of the two species show that that the intact cisplatin is excreted at much higher rate, compared to the mobile metabolite as shown in Figures 8, 11, and 17.

6.2 Promising Technique

In this thesis, pharmacokinetics (PK) of cisplatin has been investigated by using physiologically based pharmacokinetic (PBPK) technique in a relation to developing and validating PBPK model for rats and humans. Reliability of the PBPK model has been assessed by evaluating the predictive performance based on observed PK datasets which followed various administration protocols. The PBPK model of cisplatin was able to closely predict and characterize the PK behavior of cisplatin and its metabolites in plasma in rats and humans. The PBPK modelling workflow presented in this thesis provides a means for understanding kinetics characteristics of cisplatin, which might be useful for understanding and/or predicting the PK of cisplatin-analogues in future studies.

References

1. L Kelland (2007) The resurgence of platinum-based cancer chemotherapy. Nature Reviews Cancer, 7(8), 573–584

2. S Dasari, PB Tchounwou (2014) Cisplatin in cancer therapy: molecular mechanisms of action, Eur J Pharmacol. 2014 October 5; 0: p364–378

3. NJ Vogelzang, JJ Rusthoven, J Symanowski, et al. (2003) Phase III study of pemetrexed in combination with cisplatin versus cisplatin alone in patients with malignant pleural mesothelioma. J Clin Oncol; 21: 2636–2644.

4. R Mastrangelo, A Tornesello, R Riccardi, A Lasorella, S Mastrangelo, A Mancini, V Rufini, L Troncone (1995) A new approach in the treatment of stage IV neuroblastoma using a combination of [131I]meta-iodobenzylguanidine (MIBG) and cisplatin, European Journal of Cancer, 31 (4) , pp. 606-611.

5. LH Einhorn (2002) Curing metastatic testicular cancer, Proceedings of the National Academy of Sciences, 99 (7) 4592-4595

6. QB Lu, S Kalantari, CR Wang (2007) Electron Transfer Reaction Mechanism of Cisplatin with DNA at the Molecular Level. MOLECULAR PHARMACEUTICS VOL. 4, NO. 4, 624-628

7. J Faig, M Haughton, RC Taylor, RB D'Agostino, MJ Whelen, KA Porosnicu Rodriguez, M Bonomi, M Murea, M Porosnicu (2018) Retrospective analysis of cisplatin nephrotoxicity in patients with head and neck cancer receiving outpatient treatment with concurrent high-dose cisplatin and radiotherapy. Am. J. Clin. Oncol.;41(5):432-440

8. P Espié, D Tytgat, ML Sargentini-Maier, I Poggesi, JB Watelet (2009) Physiologically based Pharmacokinetic (PBPK), Drug Metabolism Reviews, 41:3, 391-407

9. Open systems pharmacology (2019) PK-Sim and MoBi, GitHub Inc, open-systems-pharmacology.org

10. A Rohatgi (2019) WebPlotDigitizer, Ankit Rohatgi, automeris.io/WebPlotDigitizer

11. AR Maharaj, AN Edginton (2014) Physiologically Based Pharmacokinetic Modeling and Simulation in Pediatric Drug Development, CPT: Pharmacometrics & Systems Pharmacology, 3, e148; doi:10.1038/psp.2014.45

12. National Center for Biotechnology Information. (2019) PubChem Database. CID=84691, https://pubchem.ncbi.nlm.nih.gov/compound/84691

13. Chemicalize, ChemAxon (https://www.chemaxon.com)

14. C Hansch, A Leo, DH Hoekman (1995) Exploring QSAR: Hydrophobic, electronic, steric constants, Washington, DC : American Chemical Society

15. PT Daley-Yates, DC McBrien (1984) Cisplatin metabolites in plasma, a study of their pharmacokinetics and importance in the nephrotoxic and antitumour activity of cisplatin, Biochemical pharmacology, vol. 33, No. 19, p. 3063-3070

16. M Verschraagen, E Boven, R Ruijter, K Born, J Berkhof, FH Hausheer, WJF Vijgh (2003) Pharmacokinetics and preliminary clinical data of the novel chemoprotectant BNP7787 and cisplatin and their metabolites, Clinical Pharmacology & Therapeutics Vol 74, 2, p157-169

17. N Nagai, K Hotta, H Yamamura, H Ogata (1995) Effects of sodium thiosulfate on the pharmacokinetics of unchanged cisplatin and on the distribution of platinum species in rat kidney: protective mechanism against cisplatin nephrotoxicity, Cancer Chemother Pharmacol 36: p404-410

18. N Nagai, M Kinoshita, H Ogata, D Tsujino, Y Wada, K Someya, T Ohno, K Masuhara, Y Tanaka, K Kato, H Nagai, A Yokoyama, Y Kurita (1996) Relationship between pharmacokinetics of unchanged cisplatin and nephrotoxicity after intravenous infusions of cisplatin to cancer patients. Cancer Chemother Pharmacol 39(1–2):131–137

19. PT Daley-Yates, DC Mcbrien (1983) Cisplatin metabolites: A method for their separation and for measurement of their renal clearance in vivo, Biochemical pharmacology, Vol 32, No 1, p181-184

20. K Hanada, K Ninomiya, H Ogata (2000) Pharmacokinetics and Toxicodynamics of Cisplatin and Its Metabolites in Rats: Relationship between Renal Handling and Nephrotoxicity of Cisplatin, J. Pharm. Pharmacol. 52: 1345-1353

21. WC Cole, W Wolf (1980) Preparation and metabolism of a cisplatin/serum protein complex, Chem. Biol. Interact., 30: 223-235

22. WC Cole, W Wolf (1981) Renal toxicity studies of protein-bound platinum(cis), Chem. Biol. Interact, 35:341-348

23. K Takahashi, T Seki, K Nishikawa, S Minamide, M Iwabuchi, M Ono, S Nagamine, H Horinishi (1985) Antitumor activity and toxicity of serum protein-bound platinum formed from cisplatin, Jpn J Cancer Res. Jan;76(1):68-74

24. WW Alden, AJ Repta (1984) Exacerbation of cisplatin-induced nephrotoxicity by methionine, Chem. Biol. Interact. 48, 121-124

25. A Mandic, J Hansson, S Linder, MC Shoshan (2003) Cisplatin induces endoplasmic reticulum stress and nucleus-independent apoptotic signaling, J Biol Chem.278(11):9100-9106

26. MA Basinger, MM Jones, MA Holscher (1990) L-Methionine antagonism of cis-platinum nephrotoxicity, Toxicol. Appl. Pharmacol. 103:   p1-15

27. PM Deegan, IS Pratt, MP Ryan (1994) The nephrotoxicity, cytotoxicity and renal handling of a cisplatinmethionine complex in male Wistar rats. Toxicology 89: p1-14

28. P Mistry, C Lee, DCH McBrien (1989) Intracellular metabolites of cisplatin in the rat kidney, Cancer Chemother Pharmacol (1989) 24: p73-79

29. RB Martin (1999) Platinum complexes: hydrolysis and binding to N(7) and N(1) of purines, In Cisplatin: Chemistry and Biochemistry of a Leading Anticancer Drug, ed. B Lippert, pp. 183–205. Weinheim, Ger.: Wiley-VCH

30. T Yotsuyanagi, M Usami, Y Noda, M Nagata (2002) Computational consideration of cisplatin hydrolysis and acid dissociation in aqueous media: effect of total drug concentrations. International Journal of Pharmaceutics 246, p95–104

31. T Zimmermann, JV Burda (2010) Cisplatin Interaction with Amino Acids Cysteine and Methionine from Gas Phase to Solutions with Constant pH, Interdiscip Sci Comput Life Sci 2: p98–114

32. F Legendre, JC Chottard (1999) Kinetics and selectivity of DNA-platination. In: Lippert B, editor. Cisplatin, chemistry and biochemistry of leading antitumor drugs. Zurich: Wiley-VCH; p. 223-245. ISBN: 3906390209

33. Y Jung, SJ Lippard (2007) Direct Cellular Responses to Platinum-Induced DNA Damage. Chemical Reviews 107, 1387–1407.

34. SE Miller, DA House (1990) The hydrolysis products of cisdichlorodiammineplatinum(II) 3. Hydrolysis kinetics at physiological pH. Inorg. Chim. Acta 173, 53-60. (20)

35. T Ishikawa, F Aliosman (1993) Glutathioneassociated cis-diamminedichloroplatinum (II) metabolism and ATP-dependent efflux from leukemia-cellsmolecular characterization of glutathione-platinum complex and its biological significance. J Biological Chem 268, p20116–20125.

36. BJ Corden (1987) Reaction of platinum(II) antitumor agents with sulfhydryl compounds and implications for nephrotoxicity. Inorganica Chimica Acta 137: p125-130

37. PC Dedon, RF Borch (1987) Characterization of the reactions of platinum antitumor agents with biologic and nonbiologic sulfur-containing nucleophiles. Biochem. Pharmacol. 36: p1955-1964

38. C Meijer, NH Mulder, GA Hospers, DR Uges, EG de Vries (1990) The role of glutathione in resistance to cisplatin in a human small cell lung cancer cell line. Br J Cancer. Jul; 62(1): 72–77.

39. National Center for Biotechnology Information. (2019) PubChem Database. CID=312, https://pubchem.ncbi.nlm.nih.gov/compound/Chloride-ion

40. National Center for Biotechnology Information. (2019) PubChem Database. CID=124886, https://pubchem.ncbi.nlm.nih.gov/compound/Glutathione

41. National Center for Biotechnology Information. (2019) PubChem Database. CID=6137, https://pubchem.ncbi.nlm.nih.gov/compound/Methionine

42. National Center for Biotechnology Information. (2019) PubChem Database. CID=5862, https://pubchem.ncbi.nlm.nih.gov/compound/Cysteine

43. ZH Siddik, DR Newell, FE Boxall, KR Harrap (1987) The comparative pharmacokinetics of carboplatin and cisplatin in mice and rats, Biochem. Pharmacol. 36 1925-1932

44. K Fukushima, A Okada, H Oe, M Hirasaki, M Hamori, A Nishimura, N Shibata, N Sugioka (2018) Pharmacokinetic–Pharmacodynamic Analysis of Cisplatin with Hydration and Mannitol Diuresis: The Contribution of Urine Cisplatin Concentration to Nephrotoxicity, Eur J Drug Metab Pharmacokinet (2018) 43: p193–203

45. A Okada, K Fukushima, M Fujita, M Nakanishi, M Hamori, A Nishimura, N Shibata, N Sugioka (2017) Alterations in Cisplatin Pharmacokinetics and Its Acute/Sub-chronic Kidney Injury over Multiple Cycles of Cisplatin Treatment in Rats, Biol. Pharm. Bull. 40, 1948–1955 (2017)

46. National Center for Biotechnology Information. (2019) PubChem Database. CID=23939, https://pubchem.ncbi.nlm.nih.gov/compound/Platinum

47. PT Daley-Yates, DC Mcbrien (1982) The mechanism of renal clearance of cisplatin (Cis-dichlorodiammine platinum II) and its modification by furosemide and probenecid, Biochemical pharmacology, vol. 31, No. 31, p. 2243-2246

48. K Fukushima, A Okada, K Sasaki, S Kishimoto, S Fukushima, M Hamori, A Nishimura, N Shibata, T Shirai, R Terauchi, T Kubo, N Sugioka (2016) Population PharmacokineticeToxicodynamic Modeling and Simulation of Cisplatin-Induced Acute Renal Injury in Rats: Effect of Dosing Rate on Nephrotoxicity. Journal of Pharmaceutical Sciences 105 324-332

49. N Nagai, H Ogata (1997) Quantitative relationship between pharmacokinetics of unchanged cisplatin and nephrotoxicity in rats: importance of area under the concentration-time curve (AUC) as the major toxicodynamic determinant in vivo. Cancer Chemother Pharmacol 40:11–18

50. A Andersson, J Fagerberg, R Lewensohn, H Ehrsson (1996) Pharmacokinetics of cisplatin and its monohydrated complex in humans. J. Pharm. Sci., 85: 824–827

51. U. S. Department of Health and Hum0na Services Food and Drug Administration Center for Drug Evaluation and Research (CDER) (2005) Guidance for industry: Estimating the Maximum Safe Starting Dose in Initial Clinical Trials for Therapeutics in Adult Healthy Volunteers, Office of Training and Communications Division of Drug Information, HFD-240